Molecular Phylogenetics and Evolution 173 (2022) 107516

Contents lists available at ScienceDirect

Molecular Phylogenetics and Evolution

journal homepage: www.elsevier.com/locate/ympev

Between a rock and a dry place: phylogenomics, biogeography, and systematics of ridge-tailed monitors (Squamata: Varanidae: *Varanus acanthurus* complex)

Carlos J. Pavón-Vázquez [a,*,1], Damien Esquerré [a], Alison J. Fitch [b], Brad Maryan [c], Paul Doughty [c], Stephen C. Donnellan [d,e], J. Scott Keogh [a]

[a] Division of Ecology and Evolution, Research School of Biology, Australian National University, Canberra, ACT 2601, Australia
[b] College of Science and Engineering, Flinders University, Bedford Park, SA 5042, Australia
[c] Collections & Research, Western Australian Museum, 49 Kew St, Welshpool, WA 6160, Australia
[d] School of Biological Sciences, University of Adelaide, Adelaide, SA 5005, Australia
[e] South Australian Museum, Adelaide SA 5000, Australia

ARTICLE INFO

Keywords:
Aridification
Australia
Morphometrics
Phylogeography
Refugia
Species delimitation

ABSTRACT

Genomic data are a powerful tool for the elucidation of evolutionary patterns at the population level and above. The combined analysis of genomic and morphological data can result in species delimitation hypotheses that reflect evolutionary history better than traditional taxonomy or any individual source of evidence. Here, we used thousands of single nucleotide polymorphisms, mitochondrial sequences, and comprehensive morphological data to characterize the evolutionary history of the ridge-tailed monitors in the *Varanus acanthurus* complex (*V. acanthurus*, *V. baritji*, and *V. storri*), a group of saxicolous lizards with a wide distribution in Australia, the driest vegetated continent. We found substantial genetic structure in the group and identify nine geographically clustered populations. Based on admixture patterns and species delimitation analyses we propose a taxonomic scheme that differs from current taxonomy. We consider *V. acanthurus* as monotypic, synonymize *V. baritji* with *V. a. insulanicus* (as a redefined *V. insulanicus*), elevate the subspecies of *V. storri* to full species (*V. storri* and *V. ocreatus*), and describe a new species from a previously identified center of endemism. The relationships among the species remain unresolved, likely as a result of fast speciation. Our study highlights the capability of large datasets to illuminate admixture patterns, biogeographic history, and species limits, even when phylogeny is not completely resolved. Furthermore, our results highlight the impact that the Cenozoic aridification of Australia had on saxicolous taxa and the role of mesic rocky escarpments as refugia. These habitats apparently allowed the persistence of lineages that became sources of colonization for arid environments.

1. Introduction

The increasing accessibility of large molecular datasets has revolutionized evolutionary research. These datasets have resolved long-standing questions about the tree of life (Delsuc et al., 2005), such as the broad-scale topology of challenging groups including green plants (One Thousand Plant Transcriptomes Initiative, 2019), mammals (Tarver et al., 2016), and birds (Jarvis et al., 2014). Based on a solid phylogenetic framework and accurate estimates of admixture, it is possible to gain new insight into the biogeographic history of taxa and evaluate the evolutionary relevance of geographic features (Moyle et al., 2016; Bryson et al., 2017; Rutherford et al., 2018). The improved ability to accurately characterize phylogenetic relationships, genetic structure, and gene flow can also help in the important task of species delimitation (Leaché et al., 2014; Stanton et al., 2019). When carefully analyzed and interpreted, genomic data has the potential to counter two major issues in species delimitation: the overlooking of cryptic lineages and over-splitting of genetically structured species (Chan et al., 2017; Leaché et al., 2019; Hundsdoerfer et al., 2019; Chambers and Hillis, 2020).

Despite the progress in molecular systematics, phenotypic data have remained relevant in species delimitation. The phenotype exposes selective forces and emerging properties of the genome that may otherwise

* Corresponding author.
E-mail address: cjpvunam@gmail.com (C.J. Pavón-Vázquez).
[1] Present address: Department of Biology, University of Kentucky, Lexington, KY 40506-0225, USA.

https://doi.org/10.1016/j.ympev.2022.107516
Received 13 January 2022; Received in revised form 25 March 2022; Accepted 6 April 2022
Available online 14 May 2022

be overlooked (Cadena and Zapata, 2021). Furthermore, approaches used to record and analyze morphological data have progressed in parallel to those used on molecular data. One such approach is geometric morphometrics, which records morphological data as either two or three-dimensional coordinates allowing the description and comparison of complex shapes (Adams et al., 2013). The combined use of genomic scale data and geometric morphometrics in species delimitation has increased in recent years, particularly in groups where overtly diagnosable features are scant (Noguerales et al., 2018; Chaplin et al., 2020; Esquerré et al., 2019, 2021).

Together, molecular and phenotypic data can shed light on how environmental change sorts biodiversity through space and time. Australia (Fig. 1A) has experienced dramatic changes in climate and vegetation despite minimal Pleistocene glaciation, being the flattest continent, and being comparatively stable tectonically (Blewett, 2012). After Australia separated from Gondwana and started drifting northwards in the late Mesozoic (Boger, 2011), mesic and rainforest habitats gradually contracted and aridity increased (Bowler, 1976; Byrne et al., 2008; 2011). In fact, today Australia is the second driest continent after Antarctica and arid or semi-arid conditions prevail over more than 70% of its surface (Bowler, 1976). The expansion of arid environments was temporally and spatially heterogeneous (Pepper and Keogh, 2021). Aridity increased sharply during the Miocene (Bowler, 1976; Hill et al. 1999; Martin, 2006), but major deserts and dunefields did not form until the Plio-Pleistocene (McLaren and Wallace, 2010). Furthermore, pockets of mesic habitat persisted in rocky escarpments across the continent. These regions likely acted as refugia in the face of aridification and now possess high levels of diversity and endemism (Fujita et al., 2010; Pepper et al., 2011a, 2011b; Oliver et al., 2014, 2019).

Monitor lizards (Squamata: Varanidae: *Varanus*) are a conspicuous and widespread component of the Australian terrestrial fauna. The miniaturized subgenus *Odatria* is the most diverse group of monitors in Australia, accounting for 19 of the 30 Australian species (Wilson and Swan, 2021). The ridge-tailed monitor (*V. acanthurus*) is a specialized member of *Odatria* that shelters in crevices and burrows within rocky outcrops, using its tail to block the entrance to them (Dryden, 2004).

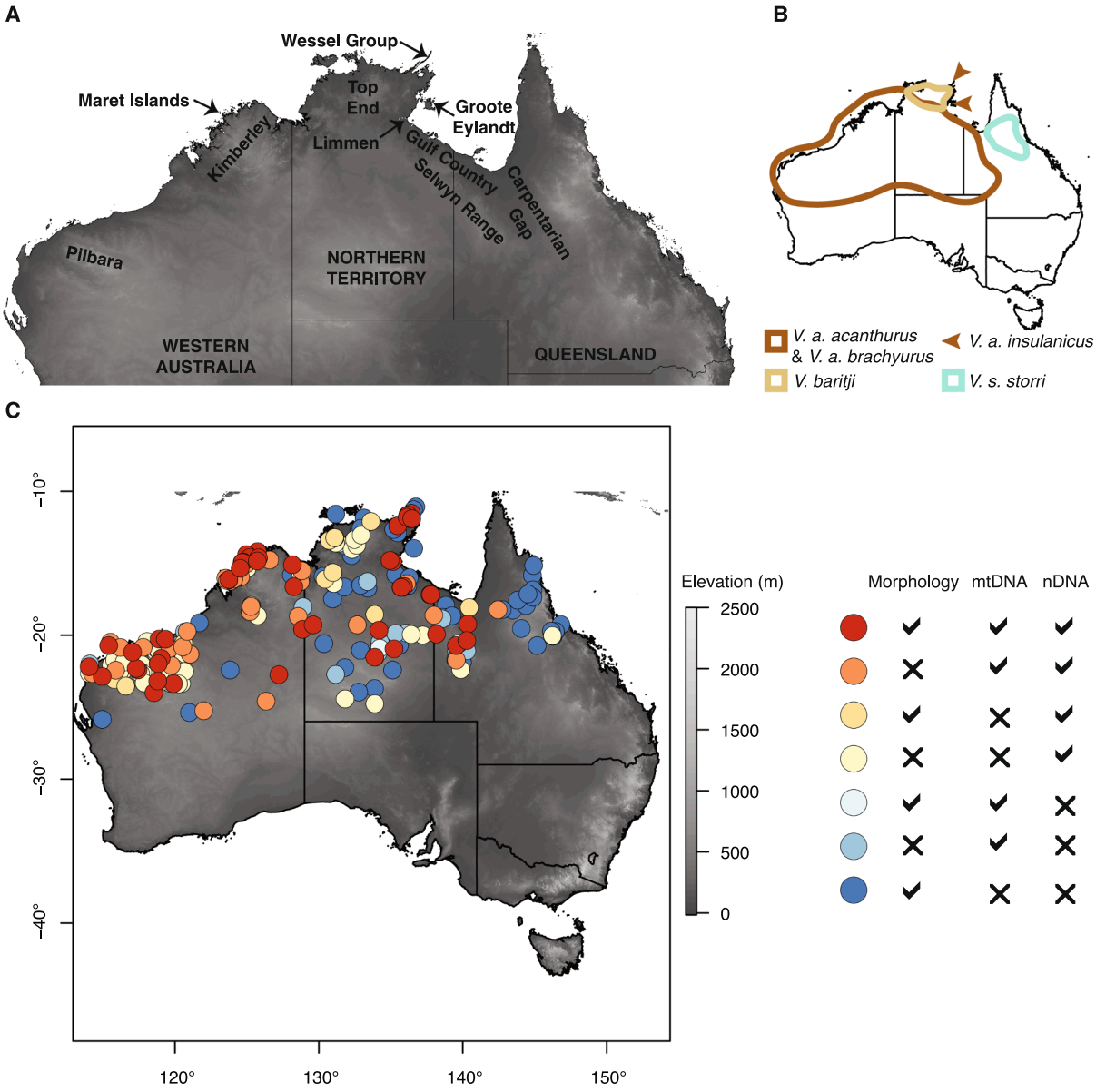

Fig. 1. Geographic setting of the present study. A) Map of northern Australia and location of areas mentioned throughout text; lines represent state/territory limits and their names are capitalized. B) Distribution of taxa in the *V. acanthurus* complex; the geographic limits of *V. a. acanthurus* and *V. a. brachyurus* are ambiguous. C) Geographic sampling of individuals in the *V. acanthurus* complex; localities are colored based on the type of data available.

Varanus acanthurus has been considered to represent either a widespread and variable species (Storr, 1980) or a species complex (King and Horner, 1987). The taxon displays considerable morphological variation throughout its wide range across the arid zone and monsoonal tropics, and this variation has been reflected in the description of three subspecies: *V. a. acanthurus* with a poorly demarcated range across monsoonal environments in the Kimberley region in northern Western Australia and surroundings; *V. a. brachyurus*, with a vaguely defined distribution encompassing a wide area in the arid and semi-arid regions of Western Australia, the Northern Territory, and Queensland; and *V. a. insulanicus*, from islands off the Northern Territory, specifically Groote Eylandt and the Wessel Group (Dryden, 2004; Cogger, 2014; Wilson and Swan, 2021) (Fig. 1B). Molecular analyses have shown that *V. a. insulanicus* is actually more closely related to *V. baritji*, from the monsoonal Top End region in the Northern Territory (Fig. 1B), than to other *V. acanthurus* (Fitch et al., 2006; Brennan et al., 2021). Furthermore, *V. storri storri* from north-eastern Queensland (Fig. 1B) appears to be more closely related to *V. acanthurus* and *V. baritji* than to *V. storri ocreatus*, from north-western Queensland, the Kimberley region, and adjacent areas in the Northern Territory (Thompson et al., 2009).

Here we use genome-wide single nucleotide polymorphisms (SNPs) and mitochondrial DNA sequences to characterize genetic population structure in ridge-tailed monitors in the *V. acanthurus* complex including the closely related *V. baritji*, and *V. s. storri*. Further, we evaluate species hypotheses derived from our molecular data with morphological traits, including geometric morphometric data. We discuss how phylogenetic relationships and geographic structure reflect past environmental change in Australia and propose a new taxonomic framework for this morphologically variable species complex.

2. Materials and methods

2.1. Molecular sampling

We genotyped individuals in the *V. acanthurus* complex using the DArTseq (Diversity Array Technology sequencing) platform designed by Diversity Arrays Technology, Canberra, Australia (DArT). This is a genome complexity reduction technique that combines fragmenting by restriction enzymes, filtering by fragment size, and sequencing (Kilian et al., 2012; Georges et al., 2018). The generated data includes thousands of fragments associated with restriction sites and their accompanying SNPs. Most fragments are 69 bp long and come from coding regions (Petroli et al., 2012). DArTseq data have proven useful to evaluate phylogeographic structure and species limits (Melville et al., 2017; Georges et al., 2018; Chaplin et al., 2020; Esquerré et al., 2021). The complexity reduction procedure was optimized for our dataset by testing different enzyme combinations, settling on PstI and SphI, and paired-end sequencing was performed in an Illumina Hiseq2500 sequencer. The genome of *V. komodoensis* (GenBank accession number SJPD00000000.1; Lind et al., 2019) was used as reference for alignment and DArT's proprietary pipelines were used to filter out bacterial contaminants.

We generated two sets of DArTseq data, given that the number of retrieved SNPs is reduced when distantly related taxa are included in the SNP calling pipeline. First, the DArT pipeline was run for 169 individuals of the *V. acanthurus* complex (*V. acanthurus*, *V. baritji*, and *V. s. storri*), obtaining a total of 202,570 SNPs. We used the 'dartR 1.8.3′ R package (Gruber et al., 2018) to filter our dataset as follows (in order). We deleted SNPs that: had a reproducibility below 0.99; were missing in more than 85% of samples; were found in the same fragment as other SNPs (to avoid linkage); or whose minor allele was found exclusively in a single individual. Subsequently, we deleted individuals with more than 70% missing data. After filtering, the dataset contained 17,277 SNPs and 162 individuals (Fig. 1C; Table S1): 144 of *V. acanthurus*, 15 of *V. baritji*, and 3 of *V. s. storri*. We used this dataset for most downstream analyses, except for those requiring outgroups, and refer to it as the population SNP dataset. The second dataset includes two individuals from each of nine populations in the *V. acanthurus* complex, one individual of *V. s. ocreatus*, two individuals of the outgroup (*V. varius*), and comprises 197,326 SNPs. We selected individuals of the *V. acanthurus* complex showing little admixture with other populations. The number of populations and admixture were estimated using the first dataset (see below). We applied the same filters specified above except for the individual filtering, obtaining 14,542 SNPs for 21 individuals (Table S1). We used this dataset in those analyses requiring outgroup specification and refer to it as the phylogenetic SNP dataset.

We also obtained partial sequences of the mitochondrial gene coding for the NADH dehydrogenase subunit 4 protein (*ND4*). Our sampling included 172 individuals (Fig. 1C; Table S1): 158 of *V. acanthurus*, 2 of *V. baritji*, 1 of *V. s. storri*, 6 of *V. s. ocreatus*, 2 each of *V. kingorum* and *V. primordius* (included here to test the relationships of *V. s. ocreatus*), and 1 of the outgroup *V. caudolineatus*. Nine sequences were obtained from GenBank, while the others were obtained following the protocol described in Fitch et al. (2006). Amplified PCR products were purified and sequenced on an AB 3730xl DNA Analyzer at the Genome Discovery Unit, ACRF Biomolecular Resource Facility, John Curtin School of Medical Research, Australian National University. We aligned the sequences using the MUSCLE algorithm (Edgar, 2004). The final alignment consisted of 600 bp.

2.2. Population structure

Analyses of population structure were performed on the population SNP dataset. First, we estimated ancestry coefficients using sNMF (Frichot et al., 2014). This is a computationally efficient but accurate method based on sparse nonnegative matrix factorization and least-squares optimization (Frichot et al., 2014). We ran the analyses on the 'LEA 2.8.0' R package (Frichot and François, 2015). First, we tested 18 combinations of the regularization (α) and tolerance (ε) parameters, choosing that with the lowest cross-entropy. In these test runs, we performed ten repetitions for each value of K (number of populations) between one and ten. We then performed 100 repetitions for each of the aforementioned values of K with the best combination of α (100) and ε (0.0001). We obtained the optimal value of K and individual ancestry coefficients from the run with the lowest cross-entropy. We also characterized population structure by performing principal component analysis (PCA) with the "gl.pcoa" function of 'dartR'.

Isolation by distance (IBD), where populations/individuals become increasingly divergent with geographic distance, appears to be common in nature (Sexton et al., 2014). We characterized patterns of IBD by evaluating the correlation between geographic and genetic distance. We measured geographic distance as the natural logarithm of the Euclidean distance between collecting localities in the Mercator projection using the 'dismo 1.1.4′ R package (Hijmans et al. 2017). Analyses of IBD usually employ $F_{ST}/1 - F_{ST}$ as measure of genetic distance, but in our study most localities are represented by a single individual. Thus, we calculated the more appropriate $\hat{a}$ statistic in Genepop v. 1.1.7 (Rousset, 2000) and used it as our measure of genetic distance (Rousset, 2000). We then performed a Mantel test to evaluate the correlation between geographic and genetic distance using the "gl.ibd" function of the 'dartR' package. We performed this test on all the samples together and independently on three sets of samples identified by sNMF that cluster together on the PCA.

2.3. Phylogenetics

We reconstructed an individual-level phylogeny of the *V. acanthurus* complex based on the SNP data through two approaches: maximum likelihood analysis of the concatenated SNPs and quartet analysis based on the coalescent. Analyses including an outgroup (*V. varius*) resulted in clade relationships that were consistent with the topology of a species tree obtained through Bayesian analysis under the multi-species

coalescent (see below). However, the number of recovered SNPs was drastically reduced to 1,041 when including the outgroup. Thus, we based the analyses on the population SNP dataset (17,277 SNPs) and rooted the tree based on the preliminary individual-level analyses that were rooted on the outgroup and the Bayesian species tree. We ran the maximum likelihood analysis on IQ-TREE 1.6.8 (Nguyen et al., 2015). We randomly assigned one or other allele for heterozygous positions and deleted 146 sites that were rendered invariable in the process. We evaluated models that incorporate ascertainment bias correction (Lewis, 2001) with ModelFinder (Kalyaanamoorthy et al., 2017) and executed the analysis under the TVM + F + ASC + R5 model, which was selected based on the Bayesian information criterion (BIC). We obtained support values through 1,000 ultrafast bootstrap replicates (Hoang et al., 2018). We performed analyses under the coalescent using SVDquartets (Chifman and Kubatko, 2014) as implemented in PAUP* 4.0 (Swofford, 2003). We used ambiguity codes for heterozygous sites and obtained support values through 1,000 bootstrap replicates.

We reconstructed the relationships between the populations in the *V. acanthurus* complex by building species trees using two approaches: quartet analysis and Bayesian estimation under the multi-species coalescent. We performed both analyses on the phylogenetic SNP dataset, assigning individuals to the populations identified by sNMF, and rooting the trees on *V. varius*. We used SVDquartets to obtain a species tree through quartet analysis, using ambiguity codes for heterozygous sites and obtaining support values through 1,000 bootstrap replicates. We performed Bayesian inference under the multi-species coalescent with SNAPP (Bryant et al., 2012) as implemented in BEAST 2.5.1 (Bouckaert et al., 2014). Just like for IQ-TREE, we randomly resolved heterozygous positions and deleted 35 sites rendered invariable. After dropping sites with missing data for one or more species, 2,361 SNPs were retained. We used a ruby script to instruct SNAPP to estimate divergence dates and specified a neighbor-joining tree obtained with the "gl.tree.nj" function of 'dartR' as starting tree (Stange et al., 2018). We applied a secondary calibration for the root age, specifying a normal distribution prior with a mean of 20.56 Ma and standard deviation of 1.5 Ma based on Brennan et al. (2021). We performed two independent analyses with 500,000 generations sampled every 250 generations. We used Tracer 1.6 (Rambaut et al., 2014) to verify convergence, that the effective sample size was above 200 for all parameters, and to determine a 10% burn-in. We combined the runs and obtained the maximum clade credibility (MCC) tree with mean node heights.

Finally, we obtained the mitochondrial tree through maximum likelihood with IQ-TREE. We used PartitionFinder 2 (Lanfear et al., 2017) to identify the best fitting codon partitioning scheme and substitution model based on the BIC. We obtained support values through 1,000 ultrafast bootstrap replicates (Hoang et al., 2018) and rooted the tree with *V. caudolineatus*.

2.4. Species concept

We adopted the general lineage species concept defining species as independently evolving metapopulation lineages (De Queiroz, 1998, 2007). Our taxonomic recommendations consider both molecular and morphological evidence. Particularly, we evaluated species limits between populations/metapopulations by testing for: fixed allelic differences, which are considered strong indicators of restricted gene flow (Georges et al., 2018), genetic divergence while accounting for incomplete lineage sorting (Jackson et al., 2017; Leaché et al., 2019), and morphometric differentiation (which indicates restricted gene flow and/or ecological divergence) (Esquerré et al., 2019). We also considered the geographic patterns of admixture obtained with sNMF. We regard sympatry or close proximity of individuals belonging to different populations—without evidence of admixture—as supporting species-level divergence, same as the geographically restricted distribution of hybrids associated with a contact zone (i.e., a hybrid zone). In contrast, we regard geographic clines of admixture (where one genetic cluster gradually gives way to another) as consistent with a single species with geographic structure but ultimately unified by extensive gene flow (Chambers and Hillis, 2020; Marshall et al., 2021).

2.5. Molecular species delimitation

We evaluated whether there are fixed differences in the population SNP dataset between the populations identified by sNMF. Fixed differences between populations are a good indicator of reproductive isolation (Georges et al., 2018). Furthermore, fixed difference analysis allows the identification of diagnosable clusters as opposed to other delimitation approaches. We tested for significant fixed differences using the "gl.fixed.diff" function of 'dartR', which identifies diagnostic differences between pairs of operational taxonomic units (OTUs). The function then assesses the significance of the results through simulation to control for false positives arising from sampling error. In each iteration, observed allele frequency distributions at a given locus are sampled at random for each population to estimate the sampling distribution of true allele frequencies at that locus (Georges et al., 2018). We performed 1,000 simulation iterations where we identified true positives based on a threshold of 0.02 for the true minor allele frequency. We collapsed the populations that did not show significant fixed differences and considered these metapopulations as OTUs in another fixed difference analysis and as putative species in downstream analyses.

We estimated the genealogical divergence index (GDI) between the groups of populations showing fixed differences to quantify their degree of genetic divergence (Jackson et al., 2017). The GDI takes values between 0 and 1, where 0 indicates a single panmictic population and 1 indicates complete isolation between OTUs (Jackson et al., 2017). Values below 0.2 are considered as strong support for a single species, values between 0.2 and 0.7 are ambiguous, and values above 0.7 indicate strong support for species-level divergence (Jackson et al., 2017; Leaché et al., 2019). The GDI for each OTU is calculated with the formula $1 - e^{-2\tau AB / \theta A}$, where τAB is the divergence time between OTUs A and B, and θA is the effective population size of OTU A (Leaché et al., 2019). We used BPP 4.2 (Flouri et al., 2018) to obtain a posterior distribution of divergence times, ancestral population sizes, and consequently the GDI. Due to computational limits, we selected 500 loci at random from the population SNP dataset. We performed independent analyses on the topologies inferred by SVDquartets and SNAPP. Based on the genetic distances between and within putative species, we specified inverse gamma (IG) priors for the ancestral population size (θ_0; IG (3, 0.002)) and root age (τ_0; IG (3, 0.005)). We ran the MCMC for 32,000 burn-in iterations and 2,000,000 post-burn-in iterations sampled every second iteration. We analyzed the results in Tracer and accordingly deleted 75% of samples from the post-burn-in stage in the analysis based on the SNAPP topology.

2.6. Morphological sampling

We obtained four morphological datasets to evaluate whether there is phenotypic differentiation between the putative species: snout-vent length (SVL) used as proxy for size, linear morphometric data describing body shape, and geometric morphometric data describing head shape in dorsal and lateral view (Tables S2–S4). Additional details on how the data was recorded are found in the Supplementary Material. All individuals included in the morphometric analyses were adults. We recorded SVL and 17 external measurements describing body shape for 172 specimens (Fig. 1C). Additionally, we obtained photographs of the head for 169 and 170 specimens in dorsal and lateral view (Fig. 1C), respectively. SNPs and mitochondrial data were available for 50 of the examined specimens, while only one of the types of molecular data were available for 14 specimens each (Table S1).

Some body measurements could not be recorded for all individuals (e.g., individuals with incomplete tails, missing fingers), in which case we used random forest training to input missing data, since some

analyses do not allow for missing data. We performed the imputation in 'missForest 1.4' (Stekhoven and Bühlmann, 2012), including putative species, sex, and SVL as predictors. Downstream analyses of SVL were performed on the natural logarithm of SVL. For the body shape dataset, we used log-shape ratios to correct for differences in body size, which we did by calculating size as the geometric mean of all the measurements, dividing each trait by size, and obtaining the natural logarithm of the resulting ratios for downstream analyses (Mosimann, 1970).

We digitalized and processed the geometric morphometric data in 'geomorph' (Adams and Otárola-Castillo, 2013). For the dorsal view of the head, we digitized 13 landmarks and 20 semi-landmarks, sliding the semi-landmarks based on the minimization of bending energy (Fig. S1). The location of the landmarks was partly based on Openshaw and Keogh (2014). For the lateral view of the head, we digitized 10 landmarks (Fig. S1). We removed the effects of size, location, and orientation through generalized Procrustes analysis (GPA) (Gower, 1975). For the dorsal view, we took bilateral symmetry into account for the GPA and used the symmetric component of shape in subsequent analyses.

For each dataset and putative species, we used the "procD.lm" function of 'geomorph' to test for significant sexual dimorphism with 1,000 permutations. We only detected sexual dimorphism in body shape. Since our sampling is male biased, we removed the females of the putative species showing significant sexual dimorphism, resulting in a total sample size of 116 individuals.

2.7. Morphological divergence

We performed analyses of variance to test whether the putative species are morphologically divergent. For SVL and other linear measurements, we performed ANOVA and then used Tukey's honest significant differences (HSD) as post-hoc test in R 3.6.2 (R Core Team, 2019). We also performed multivariate analyses on the body

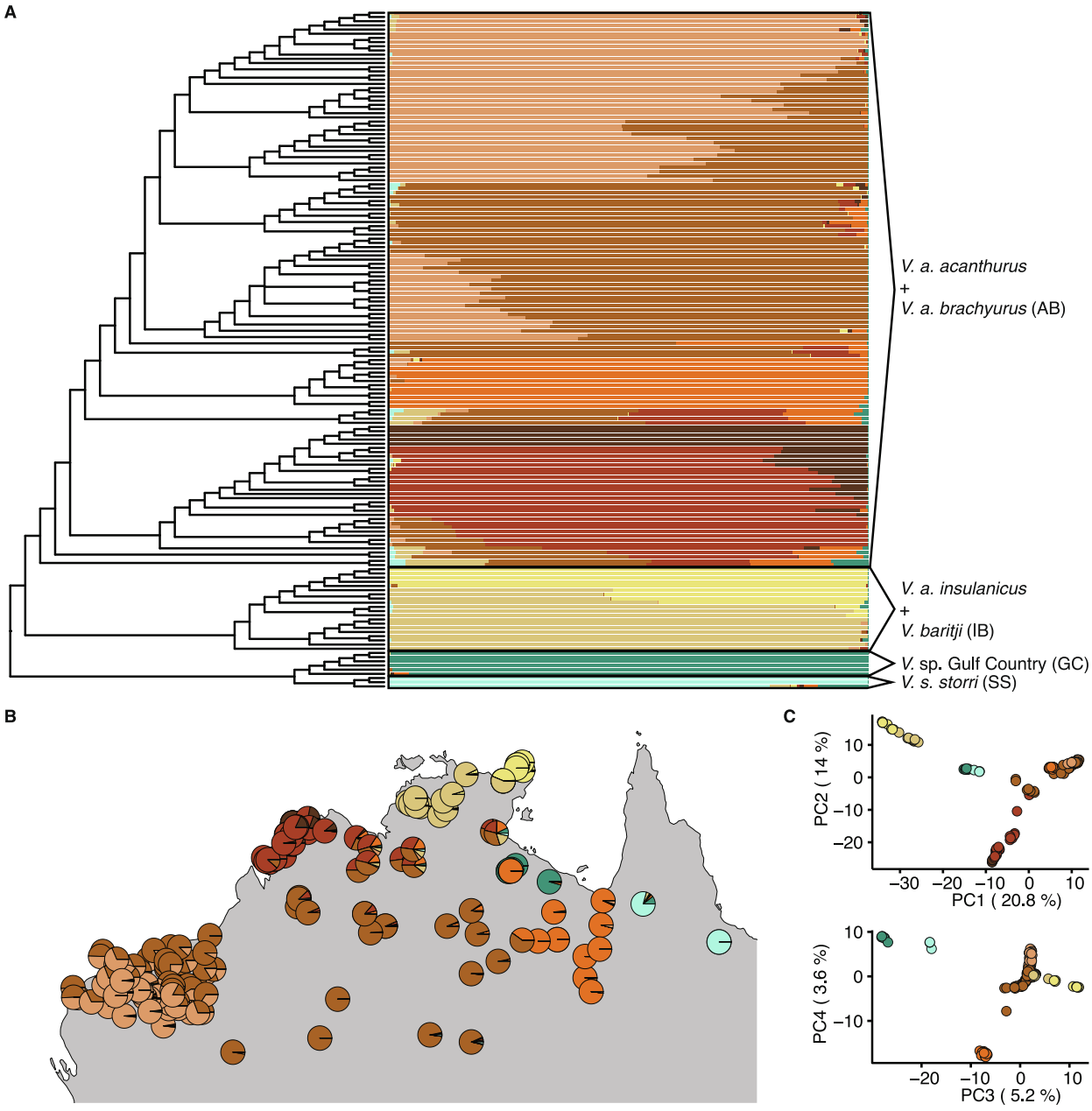

Fig. 2. Geographic structure in the *V. acanthurus* complex. A) Ancestry coefficients estimated by sNMF; the tree was obtained from the analyses of a SNP dataset with SVDquartets; branch lengths are arbitrary. B) Geographic distribution of genetic structure as inferred by sNMF; each circle represents an individual. C) Principal component analysis of the population SNP dataset; individuals are colored according to which population has the largest contribution in their ancestry coefficients.

measurements as a whole and the head shape datasets using the "advanced.procD.lm" function of 'geomorph'. We tested the influence of clade on morphological variation based on a multivariate linear model, assessing significance through 10,000 iterations. We visualized morphological differences using boxplots (SVL) and PCA plots (other datasets). Furthermore, to detect diagnostic traits we obtained scalation and coloration characters for each putative species from either the firsthand examination of specimens or the literature (Storr, 1966, 1980; King and Horner, 1987; Dryden, 2004; Eidenmüller, 2004; King, 2004; Auliya and Koch, 2020). Finally, we compiled photographs of live individuals in the *V. acanthurus* complex from throughout its range to identify consistent differences in coloration.

3. Results

3.1. Population structure

The sNMF analyses with the lowest cross-entropy were those where $K = 9$ (Fig. 2A, S2; Table S5). The distributions of three populations show broad correspondence with the known ranges of *V. s. storri*, *V. baritji*, and *V. a. insulanicus*, but some individuals in the mainland north-eastern Top End were grouped with *V. a. insulanicus* from the Top End islands (Fig. 2B). The other six populations are distributed as follows: 1) Selwyn Range, that crosses the Northern Territory-Queensland border; 2) Gulf Country; 3) widespread in the arid and semi-arid regions of central Australia; 4) Kimberley region (except for Maret Islands); 5) Maret Islands; and 6) Pilbara region (Fig. 2B). Many populations show admixture where they come into close or direct contact (Fig. 2B). Specifically, there is considerable admixture between *Varanus a. insulanicus* and *V. baritji*; between the populations in the Kimberley and Maret

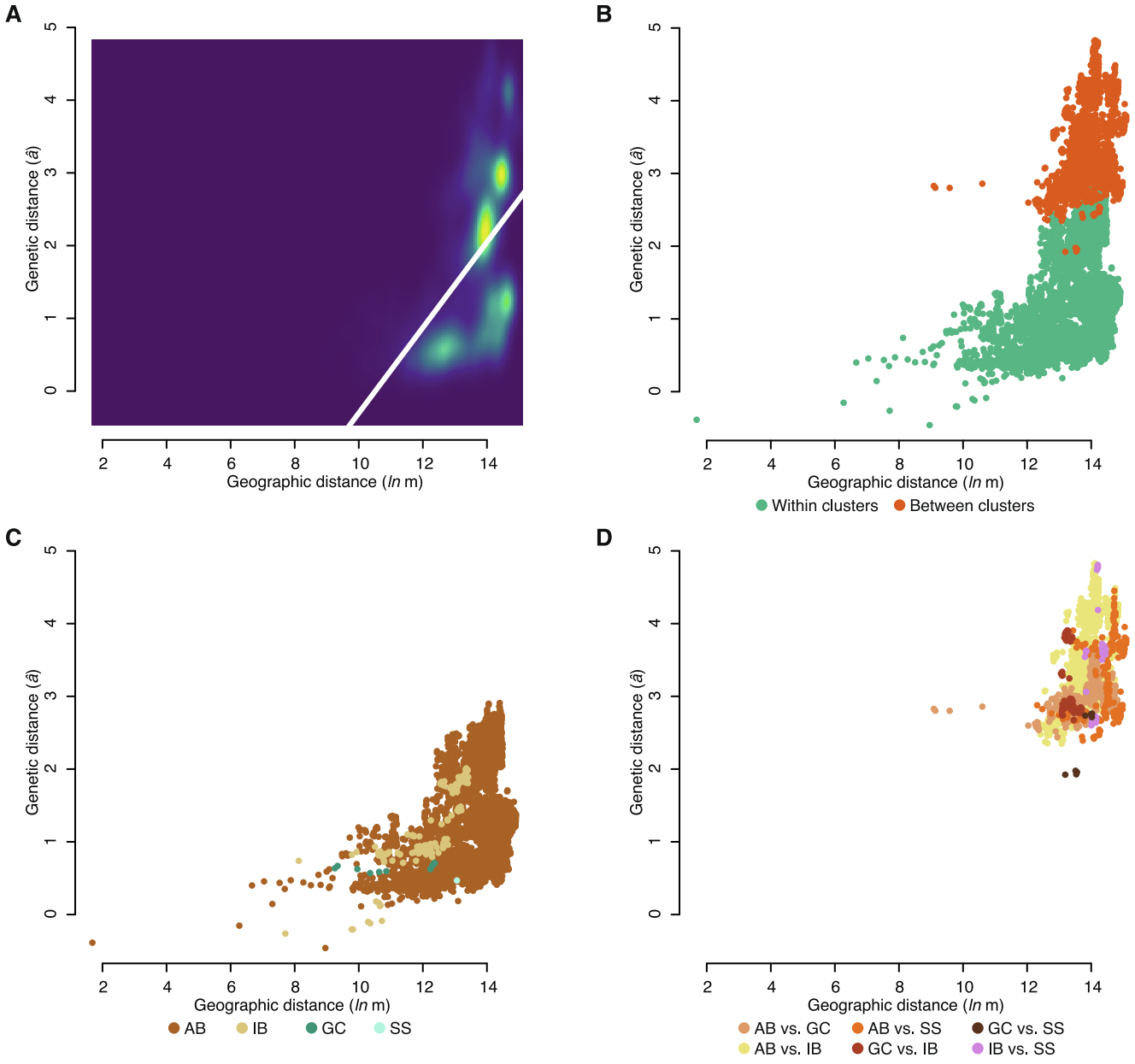

Fig. 3. Relationship between genetic and geographic distance in the *V. acanthurus* complex. Each point represents a pairwise comparison between individuals belonging to four distinct population clusters. A) Kernel density and linear regression of genetic distance against geographic distance. B) Comparison of distances within and between clusters. C) Distances within clusters. D) Distances between clusters.

Islands; and between the widespread population and the Selwyn Range, Pilbara, and Kimberley populations. Individuals from the Limmen National Park in the south-eastern Top End show mixed ancestry from several populations. Three clusters are readily identifiable in the plot of the first two PCs, which account for 20.8% and 14.0% of variation, respectively (Fig. 2C, S3). One corresponds to *V. a. insulanicus* + *V. baritji*, another to *V. s. storri* and the population from the Gulf Country, and the last one to the remaining populations. In the latter cluster, structure is apparent within the widespread and Kimberley populations. PC3, accounting for 13% of variation, more clearly distinguishes *V. s. storri* from the Gulf Country population and these two from the rest. Thus, the populations in the *V. acanthurus* complex can be grouped into four main clusters: *V. s. storri* (SS), the Gulf Country population (GC), *V. a. insulanicus* and *V. baritji* (IB), and the rest of the populations corresponding to *V. a. acanthurus* and *V. a. brachyurus* (AB).

All the Mantel tests we performed were significant, suggesting that IBD is an important driver of genetic divergence (Table S6). However, visual exploration of the data revealed that, for similar geographic distances, genetic differentiation is usually higher between the four identified clusters than within them (Fig. 3, S4). When comparing population clusters independently, we also found that for a similar geographic distance between-population genetic distance is higher than within-population distance. This suggests some degree of reproductive isolation between populations.

3.2. Phylogenetics

In the individual-level nuclear trees (Fig. 4, S5, S6), a clade that includes GC and SS appears as sister to the clade that includes AB and IB. Each of these four major clades was strongly supported, but the relationships between them are not in the SVDquartets tree. The population from the Gulf Country and *V. s. storri* were consistently recovered as sister to each other and are reciprocally monophyletic. The individuals assigned to *V. a. insulanicus* constitute a clade, but they are nested within

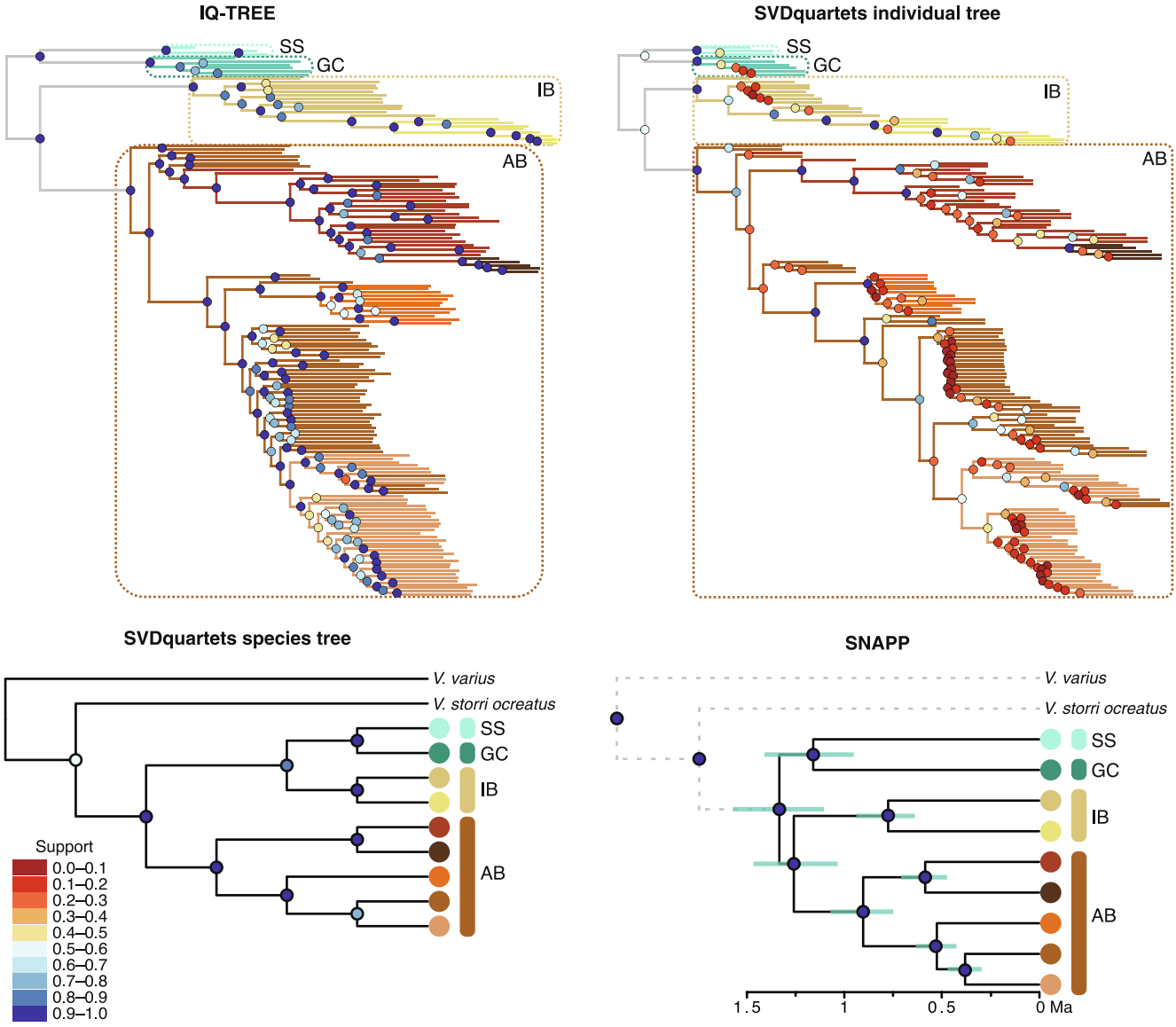

Fig. 4. Phylogenetic relationships in the *V. acanthurus* complex obtained through the analysis of SNP data. Branch lengths are arbitrary for SVDquartets, proportional to substitutions per site for IQ-TREE, and proportional to time for SNAPP. Circles in nodes indicate support values: ultrafast bootstrap for IQ-TREE, bootstrap for SVDquartets, and posterior probabilities for SNAPP. The dotted rectangles in the individual-level trees and vertical bars in the species trees indicate four major clades (see Fig. 7). In the individual-level nuclear trees, branches are colored based on their population assignment by sNMF. In the species trees, populations are indicated by the circles in the tips. In the SNAPP tree, dotted branches were shortened for visualization purposes and the horizontal blue bars indicate the 95% highest posterior density of divergence times. (For interpretation of the references to color in this figure legend, the reader is referred to the web version of this article.)

a paraphyletic *V. baritji*. Within AB, the widespread population is not monophyletic. The individuals in the Maret Islands form a clade that is nested within individuals from the Kimberley population. The Selwyn Range population is monophyletic but is nested within individuals assigned to the widespread population. The population from the Pilbara is rendered paraphyletic by a few individuals from the widespread population.

Both species trees (Figs. 4, S7) recover a monophyletic *V. acanthurus* complex to the exclusion of *V. s. ocreatus*, meaning *V. storri* is not monophyletic. The SVDquartets species tree recovers two major clades. One includes GC + SS and *V. baritji* + *V. a. insulanicus* (IB). The other clade corresponds to AB and shows the populations from the Kimberley and Maret Islands as sister to each other, and this group as sister to a clade that includes the Selwyn Range, widespread, and Pilbara populations. The latter two were recovered as sister clades. The SNAPP species tree differs by placing GC + SS as sister to AB + IB. The mean age for the most recent common ancestor (MRCA) of the *V. acanthurus* complex was 1.33 Ma (95% highest posterior density (HPD) 1.10–1.57). The deepest split between individual populations in the complex was between GC and SS (mean = 1.15 Ma, 95% HPD 0.95–1.41). The mean age of the split between AB and IB was 1.26 Ma (95% HPD 1.03–1.47). Other divergences within the complex were inferred to be more recent than 1 Ma.

The mitochondrial tree (Fig. 5, S8) also recovers a monophyletic *V. acanthurus* complex that excludes *V. s. ocreatus*. The latter appears as sister to a clade that includes the *V. acanthurus* complex and the closely related species *V. kingorum* and *V. primordius*. Within the strongly supported *V. acanthurus* complex, a clade that includes the individuals that were assigned to the *V. a. insulanicus* population by sNMF appears as sister to the rest. An individual without nuclear data but that comes from the same locality as genotyped *V. baritji* is nested within *V. a. insulanicus*. GC and SS each appear again as monophyletic and sister to each other, with AB as sister to both. Within AB, a clade that includes most of the individuals from the Kimberley and Maret Islands populations is sister to the rest. Some individuals in this clade are from the Pilbara region, and a few samples from the widespread population are nested within the Kimberley + Maret Islands clade. A clade that contains most of the individuals from the Pilbara appears as sister to a clade that includes three

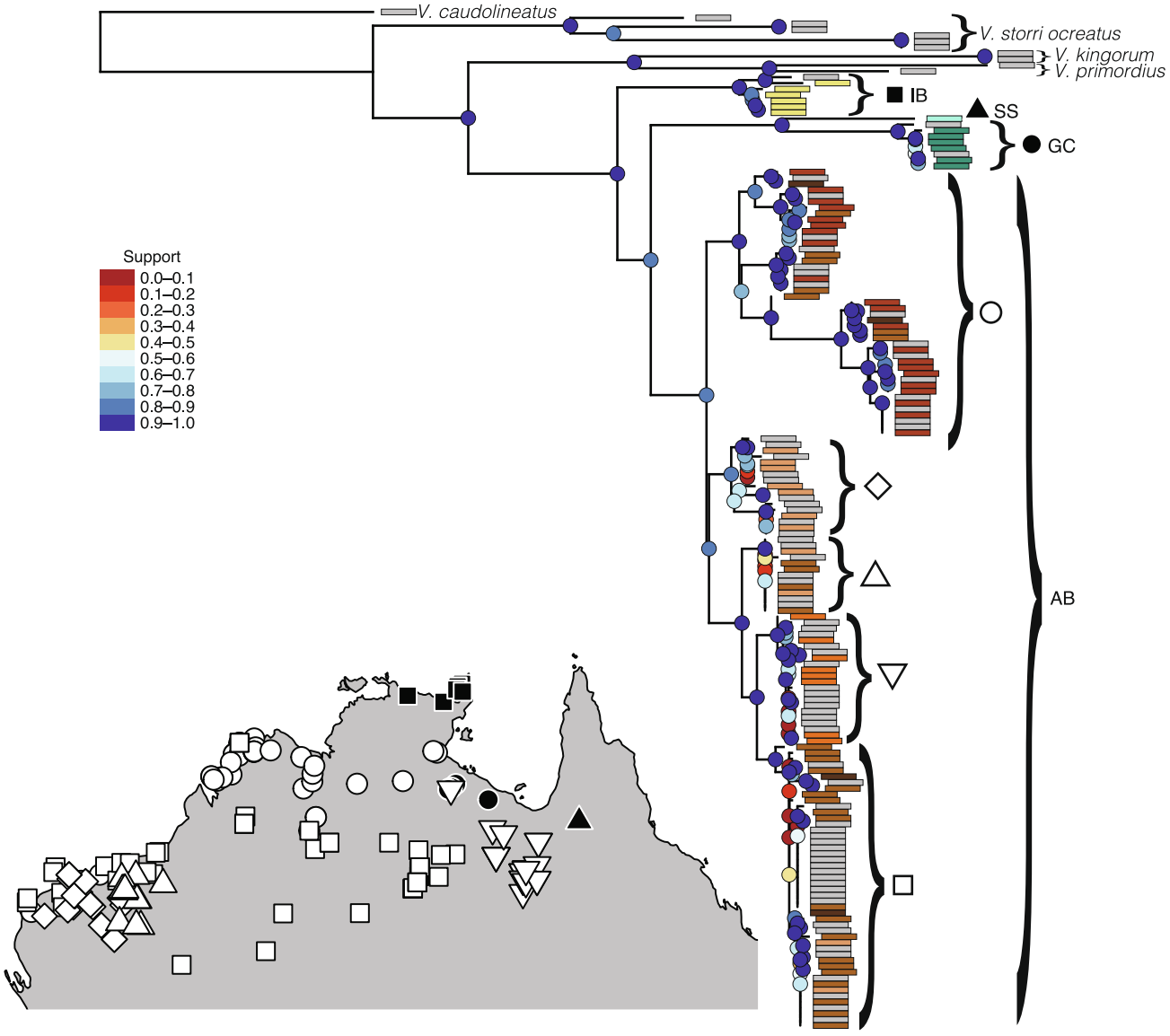

Fig. 5. Phylogenetic relationships in the *V. acanthurus* complex obtained through the analysis of mitochondrial data. The tree is a maximum likelihood phylogeny obtained with IQ-TREE. Branch lengths are proportional to substitutions per site. Circles in nodes indicate ultrafast bootstrap values. Population assignments by sNMF for individuals with SNP data are shown by the colored bars at the tips, while gray bars indicates the absence of SNP data. Symbols next to pie charts were used to map the geographic distribution of each subclade.

main subclades: one that includes individuals from the eastern Pilbara (including some that were assigned to the widespread population by sNMF), one that includes the individuals from the Selwyn Range population, and another one that includes most individuals from the widespread population plus some from the Maret Islands and the Pilbara.

3.3. Molecular species delimitation

The fixed difference analysis revealed that there are fixed differences between most populations identified by sNMF, except for the widespread and Pilbara populations (Table S7). The Gulf Country population and *V. s. storri* have significant fixed differences with each other and every other population (Fig. 6A). The differences between *V. a. insulanicus* and *V. baritji* are not significant, but each of them showed significant differences with every other population (Fig. 6A). Within AB, differences were not significant between the widespread population and every other population, except for the one from the Maret Islands. Differences were also non-significant between the Pilbara and Selwyn Range populations, and between the Kimberley and Maret Islands populations (Fig. 6A). Thus, we identified four population clusters that are likely isolated from each other (Fig. 6A). The fixed difference analysis performed on the four clusters—equivalent to AB, GC, IB, and SS, revealed significant fixed differences between them (Table S8).

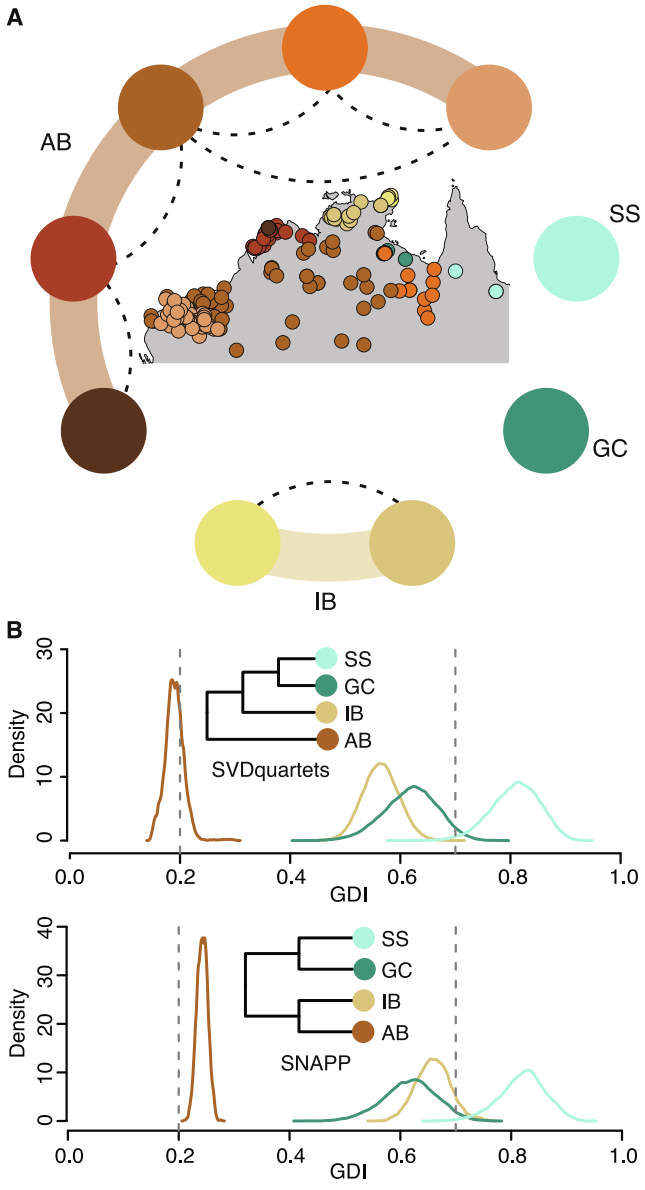

Fig. 6. Species limits in the *V. acanthurus* complex. A) Results of the fixed difference analysis; populations are indicated by circles; dotted lines connect populations with no significant fixed differences; the arched bands connect populations that are directly or indirectly connected by gene flow as suggested by the absence of significant fixed differences; i.e., putative species. B) Posterior distribution of the genealogical divergence index (GDI) between putative species; GDI values below 0.2, between 0.2 and 0.7, and above 0.7 are considered as strong evidence against species-level divergence, ambiguous, and strong evidence for species-level divergence, respectively.

The GDI suggests that the *V. acanthurus* complex comprises more than one species (Fig. 6B). We obtained similar results regardless of the topology used as input. The GDI was highest and above 0.7 for SS, supporting its species-level status. For the remaining clusters, GDI estimates are ambiguous. Among these, mean estimates are close to the upper threshold in IB and GC, and close to the lower threshold in AB.

3.4. Morphological divergence

The ANOVA coupled with HSD revealed significant differences in SVL between the following pairs of putative species (taxon with largest body size from each pair indicated by *): AB and IB* (p adjusted for multiple testing (p_{adj}) = 0.009); AB* and SS (p_{adj} = 0.002); GC and IB* (p_{adj} = 0.009); and IB* and SS (p_{adj} less than 0.0001) (Table S9). We also found significant differences between the putative species in most linear measurements describing body shape (Table S9). The closely related GC and SS significantly differ in relative head depth (p_{adj} = 0.002), hand width (p_{adj} = 0.020), toe IV length (p_{adj} = 0.040), and foot width (p_{adj} = 0.046). The multivariate analyses revealed that most taxa differ significantly in body shape, except for AB and GC (Table S9). Similarly, the PCA of the body shape variables shows that mean PC1 scores differ markedly between putative species, except for AB and GC (Fig. 7). Based on the variable contributions to PC1, individuals in SS tend to have shorter necks and longer fingers than the other taxa. On the other hand, IB individuals have longer necks and shorter fingers. PC1 scores for AB and GC are intermediate between SS and IB.

The multivariate analyses of dorsal head shape revealed that all pairs of putative species differ significantly. The PCA plot shows that individuals assigned to SS have large eyes, snouts that are short and narrow, and broad heads posteriorly (Fig. 7). The mean head shape of AB is similar, but with a narrower head posteriorly. IB has on average small eyes, a snout that is broad and long, and a narrow head posteriorly. On average, GC individuals have broad heads posteriorly and an eye length and snout shape that are intermediate between AB + SS and IB.

Lateral head shape differs significantly between the following pairs: AB-IB, AB-SS, GC-SS, and IB-SS. The PCA plot shows that individuals assigned to SS have relatively long eyes and heads that are dorsally-compressed posteriorly. On average, individuals in IB have smaller eyes and less dorsally-compressed heads. Eye length is intermediate between SS and IB in AB and GC, while they have deeper heads.

4. Taxonomy

Our taxonomic conclusions are summarized here, and the reasoning behind them is detailed in the Discussion. This article is registered in ZooBank (https://zoobank.org/60072E69-EA70-463F-9F40-2A5D46028241). Our results suggest that *V. a. insulanicus* and *V. baritji* are conspecific, and that together they represent an independent lineage within the *V. acanthurus* complex. Thus, we synonymize *V. baritji* King and Horner, 1987 with *V. a. insulanicus*. The latter has nomenclatural priority and together they represent a distinct species, *Varanus insulanicus* Mertens, 1958.

Our analyses indicate that the populations of *V. acanthurus* (i.e., the AB clade) are not genetically isolated from each other, and that together they comprise an independent evolutionary trajectory within the complex. Thus, our data demonstrate that *V. acanthurus* should be regarded

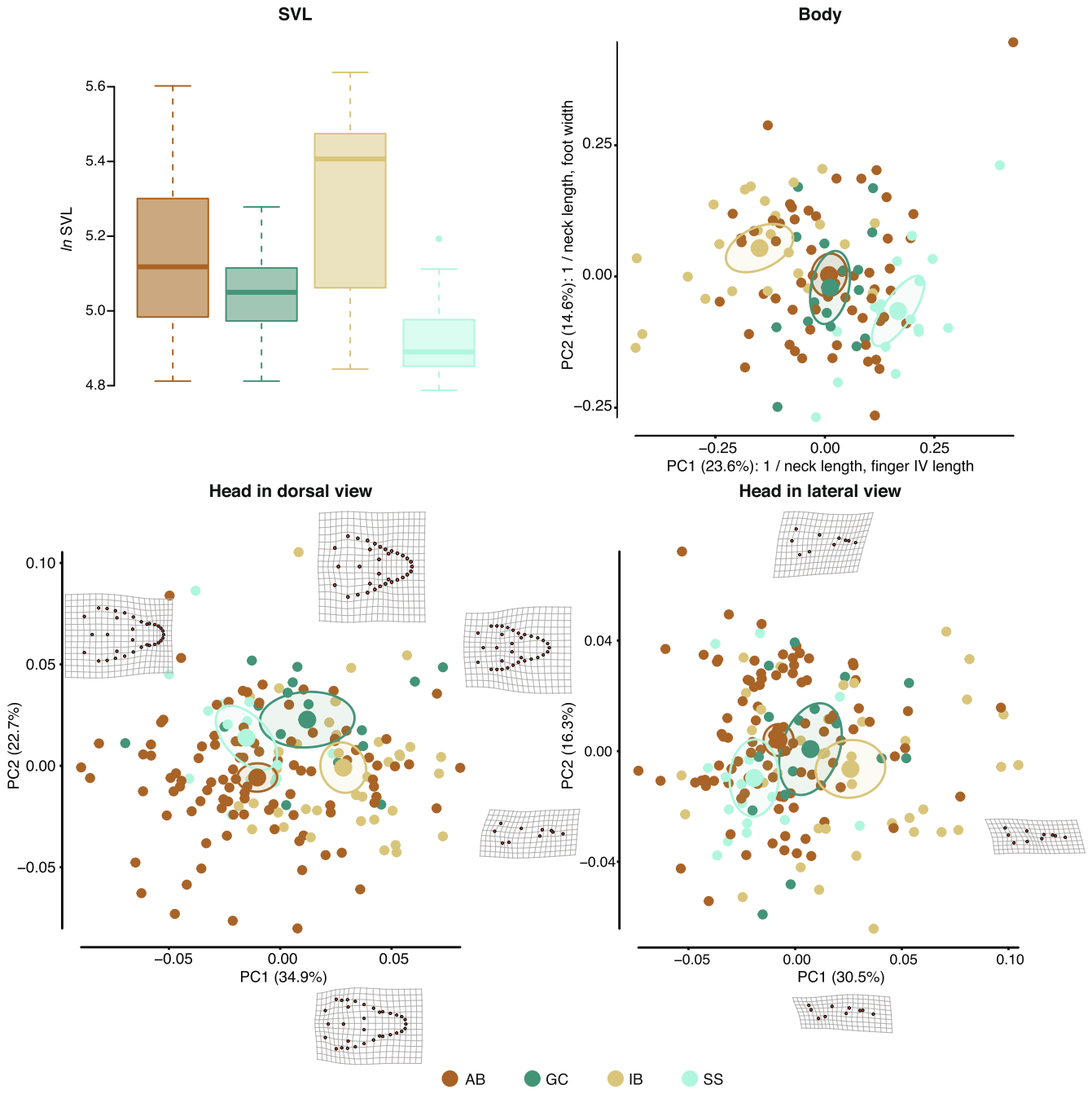

Fig. 7. Morphological variation in the *V. acanthurus* complex. Colors indicate putative species. Boxplots show variation in body size. In the principal component (PC) plots, small points represent individuals, large points represent the mean PC scores per species, and circles indicate 95% confidence ellipses. For body shape, the two variables with the greatest contribution to each PC are indicated. For head shape, the landmark configuration and deformation grids (with respect to mean shape) are shown for the individuals at the extremes of each PC.

as a monotypic and morphologically variable species.

Our trees indicate that *V. s. storri* is more closely related to species in the *V. acanthurus* complex than to *V. s. ocreatus*. Consequently, we elevate *V. s. ocreatus* to species level as *Varanus ocreatus* Storr, 1980. Finally, our results suggest that the sister lineages *V. storri* and GC are independent from each other and from other lineages in the complex. Therefore, the *V. acanthurus* complex includes four species: *V. acanthurus*, *V. insulanicus*, *V. storri*, and the GC lineage (Fig. 8). We formally describe the latter below.

5. *Varanus citrinus* sp. n.

https://zoobank.org/F2659B83-324C-4790-806E-EA1BB1C8F7CC. Figs. S9–S11, Figs. 8 and 10.

Holotype. NTM R17430. Adult male. Barney Hill, McArthur River Station, Northern Territory, Australia, 16.4167° S, 136.1000° E, 38 m elevation. Collected by N. J. Gambold on 8 October 1992.

Paratypes. Seven specimens. Australia: Northern Territory: Cape Crawford area, Barkly Tableland, 16.6000° S, 135.8850° E, 73 m elevation (NTM R20515); Cape Crawford area, Barkly Tableland, 16.6233° S, 135.7917° E, 72 m elevation (NTM R20517); Heartbreak Hotel area, 16.6833° S, 135.7167° E, 93 m elevation (NTM R20527,

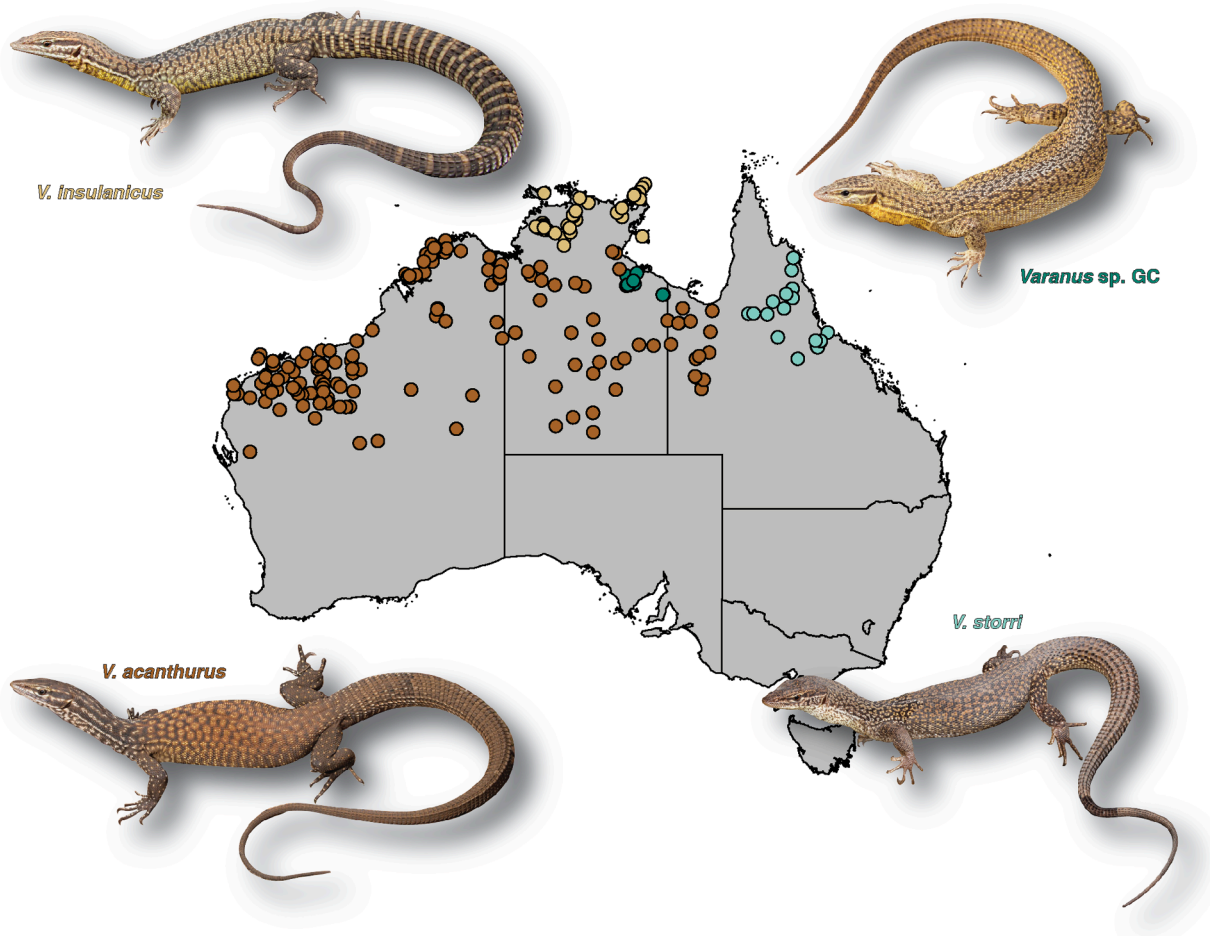

Fig. 8. Geographic distribution of species in the *V. acanthurus* complex. Only localities with sequenced or morphologically examined individuals are mapped. Lines indicate state/territory borders. Photographs by Stephen M. Zozaya.

R20529); Cape Crawford area, Barkly Tableland, 16.5967° S, 135.8933° E, 69 m elevation (NTM R20574); Cape Crawford area, Barkly Tableland, 16.6183° S, 135.8683° E, 62 m elevation (NTM R20575); Cape Crawford area, Barkly Tableland, 16.1350° S, 135.7183° E, 146 m elevation (NTM R20577).

Referred material. Eleven specimens. Australia: Northern Territory: ca. 3 km N of Amelia Spring, McArthur River, 16.5833° S, 136.1667° E, 81 m elevation (ANWC R00941); 12 km N Borroloola, 16.0000° S, 136.2833° E, 16 m elevation (AMS R.55054–R.55057); Echo Gorge Camp, Wollogorang Station, 17.1833° S, 137.7167° E, 249 m elevation (NTM R14415); Barney Hill, McArthur River Station, Northern Territory, Australia, 16.4167° S, 136.1000° E, 38 m elevation (NTM R17431); Heartbreak Hotel area, 16.6833° S, 135.7167° E, 93 m elevation (NTM R20528, R20530); Cape Crawford area, Barkly Tableland, 16.1350° S, 135.7183° E, 102 m elevation (NTM R37177); Bing Bong Station, near Borroloola, 15.6200° S, 135.3500° E, 52 m elevation (SAMA R13541); Redbank Mine, 25 km W of Wollogorang Station, 17.1800° S, 137.7700° E, 214 m elevation (SAMA R34264).

Diagnosis. A member of *Varanus* distinguished from congeners by having spinose caudal scales, the dorsal coloration consisting of an irregular dark reticulum against a pale background that gives a marbled appearance with ocelli restricted to the dorsal midline (greatly reduced in females), sexually dimorphic dorsal coloration, and a bright yellow gular region in males.

Comparisons. *Varanus citrinus* can be differentiated from most species in *Varanus* (except for *V. acanthurus*, *V. insulanicus*, *V. ocreatus*, *V. primordius*, and *V. storri*) by having spinose caudal scales (versus caudal scales smooth or weakly to strongly keeled). Distinguished from *V. acanthurus*, *V. insulanicus*, *V. ocreatus*, *V. primordius*, and *V. storri* by having the dorsal coloration consisting of an irregular dark reticulum against a pale background that gives a marbled appearance with ocelli restricted to the dorsal midline (pattern reduced in females; versus dorsal pattern consisting of regularly arranged ocelli/pale spots in *V. acanthurus* and *V. storri* (can be reduced); dark short transverse bars or reticulum (usually lacking ocelli, poorly formed at best) in *V. insulanicus*; regularly arranged reticulum usually lacking ocelli in *V. ocreatus* (can be reduced); and irregularly arranged dark and light brown speckles that sometimes are arranged into a reticulum in *V. primordius*) (Figs. 9–10); from *V. acanthurus*, *V. insulanicus*, *V. ocreatus*, and *V. primordius* by showing marked sexual dimorphism in dorsal color pattern (versus no consistent sexual dimorphism in dorsal color pattern in the other species); from *V. ocreatus*, *V. primordius*, *V. storri*, and most individuals of *V. acanthurus* by having a bright yellow gular region in males (versus gular region whitish or creamish) (Figs. 9–10); and from adult *V. acanthurus*, *V. insulanicus*, and *V. ocreatus* by having alternating dark and pale crossbands in the posterior portion of the tail (versus posterior portion of tail usually homogeneously dark in *V. acanthurus* and *V. insulanicus*, homogeneously pale or with longitudinally arranged dark markings in *V. ocreatus*) (Figs. 9–10). Additionally distinguishable from *V. acanthurus* and *V. insulanicus* by usually having fewer longitudinal scale rows at the level of the midbody (81–93, $x = 88.5$, $n = 8$; versus 82–110, $x = 99.24$, $n = 99$, in *V. acanthurus*, and 80–112, $x = 94.40$, $n = 15$, in *V. insulanicus*) (Tables S10–S11) and having dark ventral spots that end posteriorly at the level of the forelimbs (versus dark spots extending posteriorly past the vent in *V. insulanicus* and most *V. acanthurus*); additionally from *V. acanthurus* by having a broad pale vertebral stripe

Fig. 9. Morphological variation in *V. acanthurus* and *V. insulanicus*. A) Dutchess, Queensland. B) Tanami, Northern Territory (NT). C) Kaltukatjara, NT. D) Tennant Creek, NT. E) Elliot, NT. F) Indee, Western Australia (WA). G) Port Hedland, WA. H) Hamersley Ranges, WA. I) North Kimberley, WA. J–K) Adelaide River, NT. L–M) Finnis Range, NT. N) Wessell Islands, NT. All photographs by Brendan Schembri, except for I, K (Stephen M. Zozaya), and N (Nic Gambold).

in life (versus vertebral region not noticeably paler than dorsolateral region in *V. acanthurus*), and narrower transverse edges on the dorsal dark reticulum (one-scale wide; versus usually two scales wide in *V. acanthurus*) (Figs. 9–10); additionally from *V. insulanicus* by having a relatively short tail in adults (tail length/SVL ratio 1.49–1.71, $x = 1.56$, $n = 15$; versus 1.73–1.98, $x = 1.84$, $n = 18$, in *V. insulanicus*); additionally from *V. ocreatus* by having the scales on the ventral surface of the lower hindlimbs of similar size to surrounding scales (versus scales enlarged, flattened and tightly juxtaposed in *V. ocreatus*); additionally from *V. primordius* by having more longitudinal scale rows at the level of

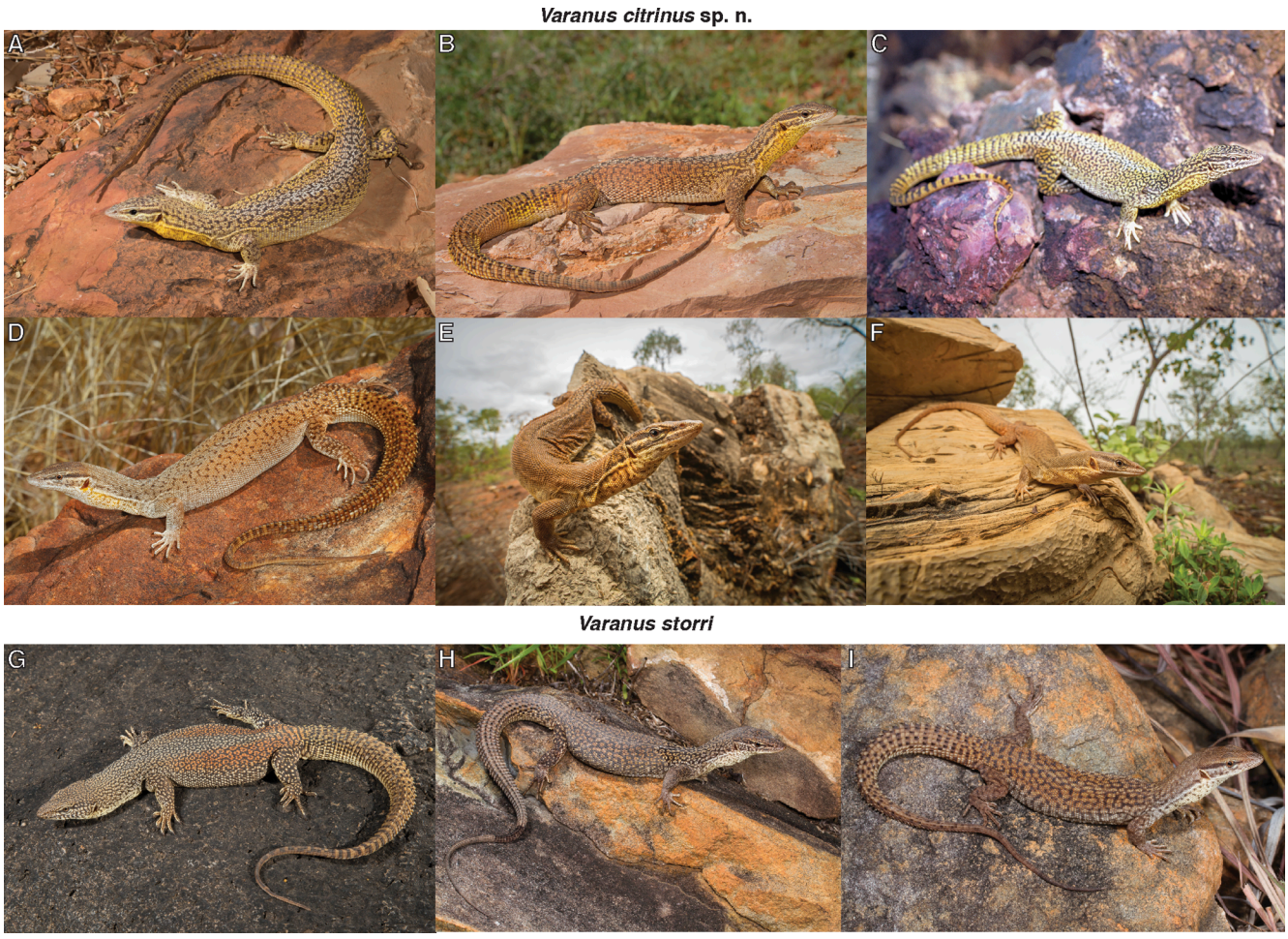

Fig. 10. Morphological variation in *V. citrinus* and *V. storri*. A–B) Cape Crawford, Northern Territory (NT). C) McArthur River Station, NT. D) Cape Crawford, NT. E–F) McArthur, NT. G) Blackbraes National Park, Queensland (QLD). H–I) Mount Carbine, Queensland. A–C are probably male, while D–F are probably female. A, H, and I by Stephen M. Zozaya. B and G by Brendan Schembri. C by Nic Gambold. D by Jules E. Farquhar. E and F by Ross McGibbon.

the midbody (81–93, $\bar{x} = 88.5$, $n = 8$; versus 60–66 in *V. primordius*) and by its larger adult size (SVL in mm 123–196, $\bar{x} = 157.38$, $n = 16$; versus 85–122, $\bar{x} = 105.16$, $n = 19$, in *V. primordius*); and additionally from *V. storri* by having more transverse rows of ventrals (57–66, $\bar{x} = 60$, $n = 8$; versus 51–54 in *V. storri*).

Description of holotype (Figs. S9–S10). Adult male. SVL 186 mm, head length 27.86 mm, head width 19.44 mm, head depth 11.02 mm, neck length 34.14 mm, body length 124 mm, hip width 16.28 mm, upper arm length 18.21 mm, lower arm length 17.88 mm, hand length 10.15 mm, hand width 8.72 mm, finger IV length 9.31 mm, upper leg length 22.81 mm, lower leg length 20.78 mm, foot length 13.86 mm, foot width 9.98 mm, toe IV length 14.64 mm, tail length 282 mm, tail width at one third of its length from vent 12.98 mm, tail depth at one third of its length from vent 10.57 mm.

Head triangular in dorsal view; temporoparietal region swollen; nuchal fold present; snout round; head profile triangular, slightly raised above nostrils; nostrils triangular, closer to tip of snout than to anterior margin of eye; canthus rostralis well-defined; tympanum higher than long, depression covered by naked skin on lower anterior margin of tympanum. Scales on dorsal surface of head flat, smooth, juxtaposed; no enlarged supraoculars, supraocular semicircles separated medially by five enlarged scales; interparietal bearing pineal eye, surrounded by eight scales; interrictals 52. Rostral larger than bordering scales; enlarged supralabials 24; enlarged loreals three, posterior loreal divided horizontally; scales in ocular region small; naked patch of skin on lower eyelid; temporal scales elongated, keeled. Mental wider than long; longitudinal mental groove between mental and level of posterior edge of eye; enlarged infralabials 24.

Nuchals elongated, domed, surrounded by granular scales; nuchals along dorsal midline between levels of posterior margin of tympanum and gular fold 32. Post-tympanic fold extending between posterior margin of tympanum and scapular region; scales around neck just anteriorly to gular fold 65. Gulars along ventral midline between mental and gular fold 63, increasing in size posteriorly; posterior gulars bearing evident sensory pits; gular fold strong, extending transversally between post-tympanic folds, bordered by small scales.

Body roughly cylindrical; dorsals elongated, domed, surrounded by granular scales; dorsals along dorsal midline between levels of gular fold and hindlimb insertion 79; scales around midbody 89. Ventrals enlarged, flat, smooth, arranged in overlapping transverse rows; ventrals along ventral midline between levels of gular fold and hindlimb insertion 57.

Limbs pentadactyl; scales on dorsal surface of limbs larger than those on ventral surface. Toe IV longest, bearing 20 rows of paired, domed subdigital scales. Claws sharp, curved, not strongly hooked.

Tail oval in cross-section anteriorly, triangular in posterior two thirds of its length. Caudal scales rectangular, strongly spinose in anterior two-thirds of tail, keeled in posterior third. Scales around tail in anteriormost complete row 48, 24 at one third of its length from vent. Lateral edges of vent surrounded by spinose scales; subcaudals enlarged, flat, smooth, arranged in overlapping transverse rows.

Color in preservative (holotype). Dorsal surface of head tan; scales

on anterior portion of head dark centered, clustering posteriorly to form irregular spots; dark semicircles above each eye; longitudinal dark stripes on parietal region. Lateral surface of head below ocular stripes cream; scales above supralabials dark centered between tip of snout and level of anterior margin of eye; discontinuous preocular stripe between nostril and eye; postocular dark stripe between eye and nuchal fold; postocular pale stripe below postocular dark stripe; scales below postocular pale stripe dark centered, dark pigment agglomerating to form irregular spots. Ventral surface of head cream, with irregular tan spots occupying between one and three scales.

Dorsal surface of neck tan; dark markings consisting of spots anteriorly, longitudinal stripes posteriorly. Lateral surface of neck cream; broken longitudinal dark stripes aligned with postocular dark stripes and dark region below postocular pale stripe, respectively. Ventral surface of neck cream, with irregular tan spots occupying between one and three scales.

Dorsal surface of body tan; vertebral pale stripe cream, around eight-scales wide at level of midbody; dorsal dark markings forming an open reticulum, giving a marbled appearance, with few ocelli that are mostly restricted to the dorsal midline. Flanks cream; dark markings of flanks conformed by vertical stripes extending from the dorsal reticulum. Ventrum cream, unpatterned except for dark spots on the chest.

Dorsal surface of limbs tan, with dark speckles that sometimes form transverse stripes on forelimbs, bearing open dark reticulum on hindlimbs. Ventral surface of limbs cream; subdigital scales dark centered.

Dorsal and lateral surfaces of tail with cream and tan speckles; dark spots transversely aligned, forming short crossbands on distal third of tail. Ventral surface of tail cream.

Color in life. This section is based on photographs of live individuals (Fig. 10). In both sexes the iris is brown and is lighter along its dorsal margin. In males, the dorsal background color ranges from light yellow to tan. The vertebral stripe is light brown or light gray. The dorsolateral region bordering the vertebral stripe is infused with either yellowish or brownish orange. The dark markings are chestnut or dark brown. The gular region posteriorly to the level of the eye is bright yellow.

In females, the dorsal background color and the vertebral stripe are either light gray or light brown. The dorsolateral region bordering the vertebral stripe is infused with brownish orange. The dorsal dark markings are totally absent or greatly reduced to form a series of disconnected lines arranged in a reticulum-like pattern. The preocular and postocular dark stripes and dark spots below it are present, as are the discontinuous lines on the neck aligned with them, but the markings on the dorsal surface of the head and neck are greatly reduced. The gular region is light gray or cream, with the yellow coloration restricted to the areas immediately below the post-tympanic fold.

Variation (Fig. S11). Morphometric data is reported in Table S2 and summarized in Tables S12 and S13. Variation on meristic scalation characters based on type series (including holotype) as follows: scales between supraorbital semicircles 4–6, $x = 5$; interrictals 48–56, $x = 52.75$; supralabials 21–26, $x = 24$; infralabials 24–30, $x = 26.88$; nuchals 32–37, $x = 33.38$; scales around neck just anteriorly to gular fold 59–73, $x = 64.63$; gulars 62–70, $x = 65.88$; dorsals 78–92, $x = 85$; scales around midbody 81–93, $x = 88.5$; ventrals 57–66, $x = 60$; paired rows of subdigital scales on toe IV 17–22, $x = 19.88$; scales around tail in anterior-most complete row 39–48, $x = 43.88$; scales around tail at one third of its length from vent 24–27, $x = 25.38$ (Table S11).

Etymology. The Latin specific epithet is treated as an adjective. *Citrinus* means "related to lemon trees", and refers to the bright yellow throats of males of the new species. We propose the common names "Gulf Ridge-tailed Monitor" or "Gulf Ridge-tailed Goanna".

Distribution and ecology. *Varanus citrinus* is only known from the basins of the McArthur and Calvert rivers. Records from each basin are separated by approximately 200 km (straight line). Additional field work and/or reappraisal of existing museum specimens is necessary to evaluate whether this gap is natural or artifactual. So far, the species is known only from the Northern Territory, but the easternmost record is 24 km (straight line) from the Queensland border.

Climate in the vicinity of the type locality is tropical monsoonal. The wet season typically takes place between December and March, with much drier conditions for the rest of the year. Vegetation is a complex mosaic of woodlands. Upland communities are found on rocky hills and dominated by *Cochlospermum* spp., *Erythrophleum chlorostachys*, *Eucalyptus leucophloia*, and *Terminalia canescens*. Lowland communities are dominated by *Corymbia terminalis*, *Eu. microtheca*, *Excoecaria parvifolia*, and *Lysiphyllum cunninghamii*. Finally, riparian communities are dominated by *Corymbia papuana* and *Melaleuca* (McArthur River Mining, 2011).

Ridge-tailed monitors are known from the Sir Edward Pellew Islands, just off the coast of the mouth of the McArthur River. These monitors could not be included in the molecular analyses, but their coloration is more similar to *V. acanthurus* than to *V. citrinus*. The closest taxonomically unambiguous records of monitors in the *V. acanthurus* complex to *V. citrinus* are those of *V. acanthurus* from McArthur, around 8 km (straight line) from a *V. citrinus* record. Other monitors that are potentially sympatric with *V. citrinus* are *V. glebopalma*, *V. gouldii*, *V. mertensi*, *V. mitchelli*, *V. ocreatus*, *V. panoptes*, *V. scalaris*, and *V. tristis* (Pianka and King, 2004).

Field notes indicate that the holotype was found "in a tree limb". Paratypes were either found on rocky outcrops, pipeline trenches, or under artificial cover (large drums). However, most of these observations come from heavily modified habitats. The extreme sexual dimorphism in dorsal and gular coloration present in *V. citrinus* warrants research into its reproductive ecology.

6. Discussion

Ridge-tailed monitors have a wide distribution in northern Australia, encompassing a variety of habitat types. Our results show that these lizards show notable geographic structure throughout their range, some of which reflects divergence at the species level. Below we focus on three aspects of the evolution of ridge-tailed monitors. First, we consider their phylogenetic relationships and likely sources of uncertainty. Second, we discuss biogeographic patterns in the group, focusing on the impacts of aridification and the role of rocky escarpments as refugia. Finally, we justify the taxonomic framework adopted in this study based on the geographic patterns of molecular and morphological variation.

6.1. Phylogeny

The employment of large molecular datasets has clarified the affinities of several taxa that were challenging to place phylogenetically based on morphology or a few loci. This has been the case of groups such as snakes (Streicher and Wiens, 2017), bats (Tsagkogeorga et al., 2013), and turtles (Chiari et al., 2012; Crawford et al., 2012). However, phylogenomic datasets have failed to unequivocally resolve phylogenetic relationships in some clades with short internodal distances, i.e., clades where divergence was fast (e.g., Burbrink et al., 2020; Morales-Briones et al., 2021). In those cases, molecular markers may not have evolved fast enough compared to reproductive isolation in order to provide sufficient phylogenetic signal (Giarla and Esselstyn, 2015; Leaché et al., 2016). Alternatively, some nodes may represent hard polytomies, with several speciation events occurring concurrently (Suh, 2016).

Some relationships in the *V. acanthurus* complex are unresolved despite the large number of loci included in this study. The SVDquartets, SNAPP, and mitochondrial topologies do not fully agree with each other. This is likely a result of the rapid and recent radiation of the *V. acanthurus* complex. The inferred dates for the splits between putative species in the complex are close to each other temporally and the credibility intervals overlap broadly. There are less than 200 kyr between the basal split in the complex and the most recent speciation event (between *V. citrinus* and *V. storri*). Alternatively, several speciation events in the group may have been quasi-simultaneous, and thus better represented

by a polytomy. Finally, phylogeny may be obscured by admixture. However, our analyses suggest that gene flow between species has been limited and all species are monophyletic in both the SNP and mitochondrial trees.

6.2. Biogeography

Despite the phylogenetic uncertainty, patterns observed in the *V. acanthurus* complex offer insight into the intricate environmental history of northern Australia. A close relationship between the complex and *V. kingorum*, *V. ocreatus*, and *V. primordius* is supported by our mitochondrial analyses and by other phylogenetic studies (e.g., Fitch et al., 2006; Vidal et al., 2012; Brennan et al., 2021). All of these taxa are distributed in the monsoonal tropics of northern Australia. *Varanus kingorum* is known from the Ord River region in Western Australia and adjacent Northern Territory; *V. ocreatus* from the Kimberley region and adjacent parts of the Northern territory, plus the semi-arid ranges in the border between the Northern Territory and Queensland; and *V. primordius* from the eastern Top End (Wilson and Swan, 2021). The *V. acanthurus* complex itself is more diverse in the monsoonal tropics, where *V. citrinus*, *V. insulanicus*, *V. storri*, and several populations of *V. acanthurus* occur. Thus, it seems likely that the *V. acanthurus* complex has a northern Australian origin.

The importance of the monsoonal tropics of Australia as a hotspot of richness and endemism is supported by studies on multiple taxa (Powney et al., 2010; González-Orozco et al., 2011; Catullo et al., 2014; Moritz et al., 2016; Braby et al., 2020), and particularly other saxicolous taxa (Potter et al., 2012; Laver et al., 2018; Esquerré et al., 2021). This is likely the result of long-term persistence in the monsoonal tropics, especially in mesic refugial areas associated with rocky escarpments in the Top End and Kimberley (Fujita et al., 2010; Laver et al., 2018; Oliver et al., 2019). Diversification of the clade including the *V. acanthurus* complex, *V. kingorum*, *V. ocreatus*, and *V. primordius* mimics that of co-distributed taxa. Diversification in the group started in the Miocene (Brennan et al., 2021) and continued into the Pleistocene, as in *Petrogale* rock wallabies (Potter et al., 2012) and multiple gecko lineages (Oliver et al., 2017). This time period in Australia is characterized by a general trend of increasing aridity and fragmentation of mesic habitats (Byrne et al., 2008; 2011), with mesic-adapted lineages becoming isolated in refugia and occasional invasion of the arid zone from the tropics (Fujita et al., 2010; Moritz et al., 2016).

Within the *V. acanthurus* complex, biogeographic patterns offer additional insight into the importance of mesic refugia in the context of aridification and the biological consequences of colonization of the Australian arid zone. Within *V. acanthurus*, endemic lineages were identified in the Kimberley, Pilbara, and Selwyn Range. These regions, with their numerous escarpments and gorges, have been previously identified as important mesic refugia in the face of increasing aridification (Fujita et al., 2010; Pepper et al., 2013; Catullo et al., 2014; Oliver et al., 2014). However, our analyses suggest that gene flow has prevented speciation of the lineages occurring there. It seems like gene flow is mainly driven by the expansion of the widespread population into the arid zone, which shows admixture with all the other populations of *V. acanthurus* with which it comes into contact. For instance, there is no significant admixture between the Pilbara population and those from the Kimberley and Selwyn Range, but there is admixture between each of these and the widespread population. Differentiation could result from the peripatric isolation of the "satellite" populations surrounding the arid zone. However, phylogenetic analyses support a northern origin of *V. acanthurus* and a recent origin of the widespread population. Furthermore, preliminary demographic analyses suggest that the widespread population experienced population expansion. Thus, it seems likely that the recent range expansion of the widespread population resulted in the reconnection of previously isolated populations. Recent evidence suggests that expansion into the arid zone may be promoting secondary contact in several Australian taxa (Pepper and Keogh, 2021). While commonly associated with rocky outcrops, *V. acanthurus* is also known to shelter in trees and burrows associated with spinifex bunchgrass (*Triodia*) wherever rocks are absent (Stammer, 1970; Swanson, 1979; Dryden, 2004). This flexibility may have enabled its range expansion into the arid zone. Colonization of surrounding habitat by lineages that are usually restricted to rocky outcrops has been observed before in lizards from northern Australia, implying that rocky refugia can be cradles of biodiversity and not just sinks (Oliver et al., 2014, 2019).

The islands off the Top End and Kimberley have been recently recognized as important centers of endemic diversity. These islands were connected to the mainland as recently as the last glacial maximum and thus the presence of endemic lineages could instead be explained by their role as refugia for previously widespread lineages (Moritz et al., 2016; Potter et al., 2016; Laver et al., 2018; Oliver et al., 2019). In the *V. acanthurus* complex, *V. insulanicus* plus the Kimberley and Maret Islands populations occur in these islands. There is some degree of differentiation between the insular and mainland populations (Fig. S3). However, gene flow has likely occurred between them and mainland populations during periods of environmental connectivity, preventing speciation. Alternatively, isolation may simply be too recent.

A wide extension of clay flats at the western base of the Cape York Peninsula, known as the Carpentarian Gap, has been demonstrated to be an important biogeographic barrier in the monsoonal tropics (Jennings and Edwards, 2005; Bowman et al., 2010; Catullo et al., 2014). Isolation between the closely related *V. citrinus* and *V. storri* seems to be driven by this break in the open woodlands of the monsoonal tropics (Catullo et al., 2014). Furthermore, the Gulf Country, where *V. citrinus* is endemic, has been recently identified as a refugium and center of endemism (Slatyer et al., 2007; Potter et al., 2016; Noble et al., 2018; Oliver et al., 2019). Endemic reptile species include the skink *Cryptoblepharus zoticus*, the gecko *Gehyra borroloola*, and the turtle *Elseya lavarackorum* (Wilson and Swan, 2021). The topographic complexity and presence of rivers and dense woodlands in the Gulf Country could explain its importance as a center of persistence in the context of aridification (Slatyer et al., 2007; Noble et al., 2018).

6.3. Systematics

Historically, species delimitation has been constrained by the adopted species concepts and the features used to define species (e.g., studies adopting the biological species concept would rely on the actual or potential production of fertile offspring to delimit species). However, it is now evident that the criteria used by each of these concepts are often violated (e.g., some deeply divergent lineages can produce fertile offspring, and not all members of a species may interbreed with each other as seen in ring species). The general lineage species concept attempts to unify the underlying rationale of previous concepts (De Queiroz, 1998, 2007). Under this framework, species are treated as hypotheses and features that would be considered as defining traits of species under other concepts, such as reproductive isolation or morphological divergence, are seen as evidence supporting the hypothesis (De Queiroz, 1998, 2007; Pante et al., 2015). In this context, our study incorporated multiple lines of evidence and relatively dense geographic sampling to develop a new taxonomic framework that reflects the evolutionary history of the *V. acanthurus* complex.

We found evidence for the conspecificity of *V. a. insulanicus* and *V. baritji*. First, there is evidence for considerable admixture between populations from the Wessel Group (formerly assigned to *V. a. insulanicus*) and mainland Top End (formerly assigned to *V. baritji*) in Donydji, in the north-eastern Top End. Additionally, they are not reciprocally monophyletic in the tree based on SNPs and we did not detect significant fixed differences between them. Morphologically, the insular individuals differ from the mainland ones by having alternating pale and dark longitudinal stripes on the neck (King and Horner, 1987). However, the transverse bars making up the dorsal pattern of insular

individuals is a more similar pattern to that of the former *V. baritji* than to other lineages in the *V. acanthurus* complex (King and Horner, 1987). Some degree of morphological differentiation in offshore island populations with small effective population sizes is not surprising (Keogh et al., 2005; Roulin and Salamin, 2010). Besides, photographic evidence provided by the Flora and Fauna Division of the Northern Territory Government indicates that individuals with a color pattern similar to that of insular lizards inhabit eastern portions of Kakadu National Park on the mainland. We could not obtain molecular data for specimens from Groote Eylandt, the type locality of *V. insulanicus* (Mertens, 1958). However, photographic evidence and our own examination of the type series show that their coloration is similar to individuals from the Wessel Group and mainland Top End. Recent speciation of the insular populations cannot be ruled out, but the evidence provided here suggests that conservatively the populations from Groote Eylandt, the Wessel Group, and mainland Top End should be considered to be conspecific under the name *V. insulanicus*. On the other hand, reciprocal monophyly, fixed allelic differences, a relatively high GDI (though inconclusive), and morphological differentiation with other taxa in the *V. acanthurus* complex suggest that *V. insulanicus* is distinct from other populations in the complex. The sNMF analysis suggests there is some admixture between *V. insulanicus* and *V. acanthurus* in the southern Top End (particularly in Limmen National Park). However, admixture seems to be geographically restricted and in the admixed individuals the genetic contribution of *V. insulanicus* is minimal compared to populations of *V. acanthurus*.

Within the complex, *V. acanthurus* has the widest distribution and notable morphological variation has been noted previously. Individuals from Barrow Island, off the coast of the Pilbara region, are miniaturized (Storr, 1980; Case and Schwaner, 1993). Individuals from the southern Pilbara are miniaturized and have a brick red background coloration. The existence of two non-sister endemic mitochondrial lineages in the Pilbara suggests there is some degree of isolation between them and with other *V. acanthurus*. However, our genomic analyses revealed that individuals from the Pilbara, including Barrow Island and the southern Pilbara, are poorly differentiated from each other and from other *V. acanthurus*. This is consistent with either very recent isolation, secondary contact, female philopatry, or a combination of these. On the other hand, individuals from the Kimberley, Maret Islands, and Selwyn Range populations have a thicker reticulum and darker coloration than other *V. acanthurus*. Some individuals in the Selwyn Range population have bright yellow gular regions, and occasionally a bright yellow dorsal background color (Schmida, 2020). However, there is considerable admixture where the different populations of *V. acanthurus* identified by sNMF come into contact, individuals assigned to the different populations interleave with each other in the nuclear and mitochondrial trees, and there are no significant fixed differences that would suggest that any population is reproductively isolated. Thus, we consider that *V. acanthurus* should be regarded as a geographically structured and morphologically variable species.

Our study confirmed that *V. storri* and *V. ocreatus* are not each other's closest relatives. In fact, our mitochondrial tree shows that *V. kingorum* and *V. primordius* are more closely related to *V. storri* than *V. ocreatus*. Morphologically, *V. ocreatus* is distinguished from *V. storri* by having enlarged scales under the distal portion of the hindlimbs, fewer scales around the midbody, fewer transverse rows of ventral scales, and a longer tail and limbs (Storr, 1980). Specimens can also be identified based on their collecting localities, as they are geographically disjunct occurring east (*V. storri*) and west (*V. ocreatus*) of the Carpentarian Gap (Wilson and Swan, 2021).

In our analyses, *V. citrinus* and *V. storri* were recovered consistently as sisters. We found that these lineages are mutually exclusive in the mitochondrial and SNP trees, show significant fixed differences, and the GDI of *V. storri* is high. Additionally, there are differences in morphometric, coloration, and scalation characters between them. Furthermore, the average uncorrected *p*-distance between these two lineages in the *ND4* alignment is 0.105, larger than the distance between other sister varanid species (Doughty et al., 2014). Finally, *V. citrinus* and *V. storri* are separated by the clay plains in the Carpentarian Gap, a well-documented biogeographic barrier (Kearns et al., 2011; Smith et al., 2011; Catullo et al., 2014). Our molecular and morphological analyses suggest that both *V. citrinus* and *V. storri* are distinct from other members of the *V. acanthurus* complex. Even when the Selwyn Range population comes close to *V. citrinus* (~8 km) in McArthur, Northern Territory, we did not find any evidence that could indicate ongoing gene flow between them, such as the detection of heavily admixed individuals or interleaving in the nuclear or mitochondrial trees. The same holds when comparing *V. insulanicus* to both *V. citrinus* and *V. storri*. Thus, we consider that *V. citrinus* and *V. storri* each represent a distinct species within the complex. Our molecular sampling of *V. storri* includes the type locality and one of the closest records to *V. citrinus*. However, we did not include records from the topographically and environmentally complex wet tropics of northeastern Queensland. Thus, the possibility that there is additional diversity within *V. storri* cannot be ruled out.

The newly acknowledged diversity of the *V. acanthurus* complex is notable given its relatively young age. Recent and rapid speciation has been inferred before in varanids, but mostly in insular radiations (Zhu et al., 2020; Pavón-Vázquez et al., 2022). The fast appearance of reproductive isolation in the *V. acanthurus* complex may be associated with the saxicolous habits of most populations in the complex, meaning that habitat fragmentation of rocky habitats can quickly lead to isolation. Ecological specialization has been shown to be positively correlated with speciation rates in both insular and continental radiations (Conway and Olsen, 2019). The appearance of traits that may be associated with assortative mating (such as sexually dimorphic coloration and brightly-colored throats) may also promote fast speciation (Hoskin, 2007), but the relationship between speciation and sexual traits is complex (Bolnick and Doebeli, 2003; Ritchie et al., 2007; Cooper et al., 2011).

7. Conclusions

Genetic structure in ridge-tailed monitors reflects the environmental change that Australia has experienced during the Quaternary, particularly the effects of aridification and the persistence of mesic pockets. Furthermore, morphological and molecular evidence together indicate that the traditional taxonomy of the group does not effectively reflect its evolutionary history. We suggest that the *V. acanthurus* complex consists of four species: *V. acanthurus*, *V. insulanicus*, *V. storri* and the newly described *V. citrinus*. Our results highlight how dense geographic and genomic sampling can illuminate patterns of isolation and contact across changing landscapes. Our study also shows how morphological data remains an essential tool in taxonomy, and how it can be used with other sources of evidence to accurately delineate natural entities.

CRediT authorship contribution statement

Carlos J. Pavón-Vázquez: Conceptualization, Methodology, Software, Formal analysis, Investigation, Writing – original draft, Visualization, Funding acquisition. **Damien Esquerré:** Methodology, Software, Formal analysis, Writing – review & editing, Visualization. **Alison J. Fitch:** Investigation, Writing – review & editing. **Brad Maryan:** Investigation, Writing – review & editing. **Paul Doughty:** Investigation, Writing – review & editing, Resources. **Stephen C. Donnellan:** Conceptualization, Investigation, Writing – review & editing, Resources. **J. Scott Keogh:** Conceptualization, Writing – review & editing, Resources, Supervision, Project administration, Funding acquisition.

Declaration of Competing Interest

The authors declare that they have no known competing financial interests or personal relationships that could have appeared to influence the work reported in this paper.

Acknowledgements

We thank A.P. Amey, R.D. Bray, P.D. Campbell, P.J. Couper, G.M. Dally, A. Drew, M.R. Hutchinson, L. Joseph, C. Kovach, S. Mahony, J. Melville, J.J.L. Rowley, J.W. Streicher, S. South, J. Sumner, A. Velasco Castrillón, and J. Worthington Wilmer for the support provided during specimen examination in their respective institutions and for the loan of tissue samples; M. Arvizu Meza, I.G. Brennan, and S. Tiatragul for their help with specimen examination; R.A. Catullo, J. Fenker, and B.Q. Minh for methodological suggestions; C. Correa Ospina, T. Cripps, A. Kilian, and M. Pepper for their help with sequencing; A. de Laive, J.E. Farquhar, N. Gambold, C.J. Jolly, R. McGibbon, B. Schembri, and S.M. Zozaya for sharing relevant photographs; J. Dobry for sharing SNP data for *V. storri*; G. Orti, R.A. Pyron and two anonymous reviewers for their pertinent comments on a previous version of this manuscript; and J. Ritchie for help when taking the photographs in Figs. S10 and S11.

Funding

This work was supported by grants from the Australian Capital Territory Herpetological Association to C.J.P.V. and the Australian Research Council to J.S.K. Support for the graduate education of C.J.P.V. was awarded by the Australian Government Research Training Program. These organizations only funded the collection of data, but they were not involved in study design, in the analysis and interpretation of data, in the writing of the report, or in the decision to submit the article for publication.

Appendix A. Supplementary material

Supplementary data to this article can be found online at https://doi.org/10.1016/j.ympev.2022.107516. DArTseq data and GenBank accession numbers of mitochondrial data are available at Zenodo (https://doi.org/10.5281/zenodo.6369188).

References

Adams, D.C., Otárola-Castillo, E., 2013. geomorph: an R package for the collection and analysis of geometric morphometric shape data. Methods Ecol. Evol. 4 (4), 393–399. https://doi.org/10.1111/2041-210X.12035.

Adams, D.C., Rohlf, F.J., Slice, D.E., 2013. A field comes of age: geometric morphometrics in the 21st century. Hystrix 24 (1), 7. https://doi.org/10.4404/hystrix-24.1-6283.

Auliya, M., Koch, A., 2020. Visual identification guide to the monitor lizard species of the world (genus *Varanus*). Bundesamt für Naturschutz (BfN), Bonn (Germany).

Blewett, R., 2012. Shaping a nation: A geology of Australia. ANU Press. http://. https://doi.org/10.22459/SN.08.2012.

Boger, S.D., 2011. Antarctica—before and after Gondwana. Gondwana Res. 19 (2), 335–371. https://doi.org/10.1016/j.gr.2010.09.003.

Bolnick, D.I., Doebeli, M., 2003. Sexual dimorphism and adaptive speciation: two sides of the same ecological coin. Evolution 57 (11), 2433–2449. https://doi.org/10.1111/j.0014-3820.2003.tb01489.x.

Bouckaert, R., Heled, J., Kühnert, D., Vaughan, T., Wu, C.-H., Xie, D., Suchard, M.A., Rambaut, A., Drummond, A.J., 2014. BEAST 2: A software platform for bayesian evolutionary analysis. PLoS Comput. Biol. 10 (4), e1003537 https://doi.org/10.1371/journal.pcbi.1003537.

Bowler, J.M., 1976. Aridity in Australia: age, origins and expression in aeolian landforms and sediments. Earth Sci. Rev. 12 (2–3), 279–310. https://doi.org/10.1016/0012-8252(76)90008-8.

Bowman, D.M.J.S., Brown, G.K., Braby, M.F., Brown, J.R., Cook, L.G., Crisp, M.D., Ford, F., Haberle, S., Hughes, J., Isagi, Y., Joseph, L., McBride, J., Nelson, G., Ladiges, P.Y., 2010. Biogeography of the Australian monsoon tropics. J. Biogeogr. 37 (2), 201–216. https://doi.org/10.1111/j.1365-2699.2009.02210.x.

Braby, M.F., Williams, M.R., Coppen, R.A.M., Williams, A.A.E., Franklin, D.C., 2020. Patterns of species richness and endemism of butterflies and day-flying moths in the monsoon tropics of northern Australia. Biol. Conserv. 241, 108357 https://doi.org/10.1016/j.biocon.2019.108357.

Brennan, I.G., Lemmon, A.R., Lemmon, E.M., Portik, D.M., Weijola, V., Welton, L., Donnellan, S.C., Keogh, J.S., 2021. Phylogenomics of monitor lizards and the role of competition in dictating body size disparity. Syst. Biol. 70 (1), 120–132. https://doi.org/10.1093/sysbio/syaa046.

Bryant, D., Bouckaert, R., Felsenstein, J., Rosenberg, N.A., RoyChoudhury, A., 2012. Inferring species trees directly from biallelic genetic markers: bypassing gene trees in a full coalescent analysis. Mol. Biol. Evol. 29 (8), 1917–1932. https://doi.org/10.1093/molbev/mss086.

Bryson Jr, R.W., Linkem, C.W., Pavón-Vázquez, C.J., Nieto-Montes de Oca, A., Klicka, J., McCormack, J.E., 2017. A phylogenomic perspective on the biogeography of skinks in the *Plestiodon brevirostris* group inferred from target enrichment of ultraconserved elements. J. Biogeogr. 44 (9), 2033–2044. https://doi.org/10.1111/jbi.12989.

Burbrink, F.T., Grazziotin, F.G., Pyron, R.A., Cundall, D., Donnellan, S., Irish, F., Zaher, H., 2020. Interrogating genomic-scale data for Squamata (lizards, snakes, and amphisbaenians) shows no support for key traditional morphological relationships. Syst. Biol. 69 (3), 502–520. https://doi.org/10.1093/sysbio/syz062.

Byrne, M., Steane, D.A., Joseph, L., Yeates, D.K., Jordan, G.J., Crayn, D., Aplin, K., Cantrill, D.J., Cook, L.G., Crisp, M.D., Keogh, J.S., Melville, J., Moritz, C., Porch, N., Sniderman, J.M.K., Sunnucks, P., Weston, P.H., 2011. Decline of a biome: evolution, contraction, fragmentation, extinction and invasion of the Australian mesic zone biota. J. Biogeogr. 38 (9), 1635–1656. https://doi.org/10.1111/j.1365-2699.2011.02535.x.

Byrne, M., Yeates, D.K., Joseph, L., Kearney, M., Bowler, J., Williams, M.A.J., Cooper, S., Donnellan, S.C., Keogh, J.S., Leys, R., Melville, J., Murphy, D.J., Porch, N., Wyrwoll, K.-H., 2008. Birth of a biome: insights into the assembly and maintenance of the Australian arid zone biota. Mol. Ecol. 17 (20), 4398–4417. https://doi.org/10.1111/j.1365-294X.2008.03899.x.

Cadena, C.D., Zapata, F., 2021. The genomic revolution and species delimitation in birds (and other organisms): Why phenotypes should not be overlooked. Ornithology 138 (2). https://doi.org/10.1093/ornithology/ukaa069.

Case, T.J., Schwaner, T.D., 1993. Island/mainland body size differences in Australian varanid lizards. Oecologia 94 (1), 102–109. https://doi.org/10.1007/BF00317309.

Catullo, R.A., Lanfear, R., Doughty, P., Keogh, J.S., 2014. The biogeographical boundaries of northern Australia: evidence from ecological niche models and a multi-locus phylogeny of *Uperoleia* toadlets (Anura: Myobatrachidae). J. Biogeogr. 41 (4), 659–672. https://doi.org/10.1111/jbi.12230.

Chambers, E.A., Hillis, D.M., 2020. The multispecies coalescent over-splits species in the case of geographically widespread taxa. Syst. Biol. 69 (1), 184–193. https://doi.org/10.1093/sysbio/syz042.

Chan, K.O., Alexander, A.M., Grismer, L.L., Su, Y.C., Grismer, J.L., Quah, E.S., Brown, R. M., 2017. Species delimitation with gene flow: A methodological comparison and population genomics approach to elucidate cryptic species boundaries in Malaysian Torrent Frogs. Mol. Ecol. 26 (20), 5435–5450. https://doi.org/10.1111/mec.14296.

Chaplin, K., Sumner, J., Hipsley, C.A., Melville, J., 2020. An integrative approach using phylogenomics and high-resolution x-ray computed tomography for species delimitation in cryptic taxa. Syst. Biol. 69 (2), 294–307. https://doi.org/10.1093/sysbio/syz048.

Chiari, Y., Cahais, V., Galtier, N., Delsuc, F., 2012. Phylogenomic analyses support the position of turtles as the sister group of birds and crocodiles (Archosauria). BMC Biol. 10 (1), 1–15. https://doi.org/10.1186/1741-7007-10-65.

Chifman, J., Kubatko, L., 2014. Quartet inference from snp data under the coalescent model. Bioinformatics 30 (23), 3317–3324. https://doi.org/10.1093/bioinformatics/btu530.

Cogger, H.G., 2014. Reptiles and amphibians of Australia, seventh ed. CSIRO publishing. https://doi.org/10.1071/9780643109773.

Conway, M., Olsen, B.J., 2019. Contrasting drivers of diversification rates on islands and continents across three passerine families. Proc. R. Soc. B. 286 (1915), 20191757. https://doi.org/10.1098/rspb.2019.1757.

Cooper, I.A., Gilman, R.T., Boughman, J.W., 2011. Sexual dimorphism and speciation on two ecological coins: patterns from nature and theoretical predictions. Evolution 65 (9), 2553–2571. https://doi.org/10.1111/j.1558-5646.2011.01332.x.

Crawford, N.G., Faircloth, B.C., McCormack, J.E., Brumfield, R.T., Winker, K., Glenn, T. C., 2012. More than 1000 ultraconserved elements provide evidence that turtles are the sister group of archosaurs. Biol. Lett. 8 (5), 783–786. https://doi.org/10.1098/rsbl.2012.0331.

De Queiroz, K., 1998. The general lineage concept of species, species criteria, and the process of speciation: a conceptual unification and terminological recommendations. In: Howard, D.J., Berlocher, S.H. (Eds.), Endless forms: species and speciation. Oxford University Press.

De Queiroz, K., 2007. Species concepts and species delimitation. Syst. Biol. 56 (6), 879–886. https://doi.org/10.1080/10635150701701083.

Delsuc, F., Brinkmann, H., Philippe, H., 2005. Phylogenomics and the reconstruction of the tree of life - Nature Reviews Genetics. Nat. Rev. Genet. 6 (5), 361–375. https://doi.org/10.1038/nrg1603.

Doughty, P., Kealley, L., Fitch, A., Donnellan, S.C., 2014. A new diminutive species of *Varanus* from the Dampier Peninsula, western Kimberley region, Western Australia. Rec. West. Aust. Mus. 29 (2), 128–140. https://doi.org/10.18195/issn.0312-3162.29(2).2014.128-140.

Dryden, G., 2004. *Varanus acanthurus*. In: Pianka, E.R., King, D.R. (Eds.), Varanoid lizards of the world. Indiana University Press.

Edgar, R.C., 2004. MUSCLE: multiple sequence alignment with high accuracy and high throughput. Nucleic Acids Res. 32 (5), 1792–1797. https://doi.org/10.1093/nar/gkh340.

Eidenmüller, B., 2004. *Varanus storri*. In: Pianka, E.R., King, D.R. (Eds.), Varanoid lizards of the world. Indiana University Press.

Esquerré, D., Donnellan, S.C., Pavón-Vázquez, C.J., Fenker, J., Keogh, J.S., 2021. Phylogeography, historical demography and systematics of the world's smallest pythons (Pythonidae, *Antaresia*). Mol. Phylogenet. Evol. 161, 107181 https://doi.org/10.1016/j.ympev.2021.107181.

Esquerré, D., Ramírez-Álvarez, D., Pavón-Vázquez, C.J., Troncoso-Palacios, J., Garín, C. F., Keogh, J.S., Leaché, A.D., 2019. Speciation across mountains: Phylogenomics, species delimitation and taxonomy of the *Liolaemus leopardinus* clade (Squamata, Liolaemidae). Mol. Phylogenet. Evol. 139, 106524 https://doi.org/10.1016/j.ympev.2019.106524.

Fitch, A.J., Goodman, A.E., Donnellan, S.C., 2006. A molecular phylogeny of the Australian monitor lizards (Squamata : Varanidae) inferred from mitochondrial DNA sequences. Aust. J. Zool. 54 (4), 253–269. https://doi.org/10.1071/ZO05038.

Flouri, T., Jiao, X., Rannala, B., Yang, Z., 2018. Species tree inference with BPP using genomic sequences and the multispecies coalescent. Mol. Biol. Evol. 35 (10), 2585–2593. https://doi.org/10.1093/molbev/msy147.

Frichot, E., François, O., 2015. LEA: An R package for landscape and ecological association studies. Methods Ecol. Evol. 6 (8), 925–929. https://doi.org/10.1111/2041-210X.12382.

Frichot, E., Mathieu, F., Trouillon, T., Bouchard, G., François, O., 2014. Fast and efficient estimation of individual ancestry coefficients. Genetics 196 (4), 973–983. https://doi.org/10.1534/genetics.113.160572.

Fujita, M.K., McGuire, J.A., Donnellan, S.C., Moritz, C., 2010. Diversification and persistence at the arid–monsoonal interface: Australia-wide biogeography of the Bynoe's Gecko (*Heteronotia binoei*; Gekkonidae). Evolution 64 (8), 2293–2314. https://doi.org/10.1111/j.1558-5646.2010.00993.x.

Georges, A., Gruber, B., Pauly, G.B., White, D., Adams, M., Young, M.J., Kilian, A., Zhang, X., Shaffer, H.B., Unmack, P.J., 2018. Genomewide SNP markers breathe new life into phylogeography and species delimitation for the problematic short-necked turtles (Chelidae: *Emydura*) of eastern Australia. Mol. Ecol. 27 (24), 5195–5213. https://doi.org/10.1111/mec.14925.

Giarla, T.C., Esselstyn, J.A., 2015. The challenges of resolving a rapid, recent radiation: empirical and simulated phylogenomics of Philippine shrews. Syst. Biol. 64 (5), 727–740. https://doi.org/10.1093/sysbio/syv029.

González-Orozco, C.E., Laffan, S.W., Miller, J.T., 2011. Spatial distribution of species richness and endemism of the genus *Acacia* in Australia. Aust. J. Bot. 59 (7), 601–609. https://doi.org/10.1071/BT11112.

Gower, J.C., 1975. Generalized procrustes analysis. Psychometrika 40 (1), 33–51. https://doi.org/10.1007/BF02291478.

Gruber, B., Unmack, P.J., Berry, O.F., Georges, A., 2018. DARTR: An R package to facilitate analysis of SNP data generated from reduced representation genome sequencing. Mol. Ecol. Resour. 18 (3), 691–699. https://doi.org/10.1111/1755-0998.12745.

Hijmans R. J., Phillips, S., Leathwick, J., & Elith, J. (2017). dismo: Species Distribution Modeling. Available at: https://CRAN.R-project.org/package=dismo.

Hill, R.S., Truswell, E.M., McLoughlin, S., Dettman, M.E., 1999. The evolution of the Australian flora: fossil evidence. In: Orchard, A.E. (Ed.), Flora of Australia. CSIRO Publishing, Melbourne, Australia, pp. 251–320.

Hoang, D.T., Chernomor, O., von Haeseler, A., Minh, B.Q., Vinh, L.S., 2018. UFBoot2: Improving the ultrafast bootstrap approximation. Mol. Biol. Evol. 35 (2), 518–522. https://doi.org/10.1093/molbev/msx281.

Hoskin, C.J., 2007. Description, biology and conservation of a new species of Australian tree frog (Amphibia: Anura: Hylidae: *Litoria*) and an assessment of the remaining populations of *Litoria genimaculata* Horst, 1883: systematic and conservation implications of an unusual speciation event. Biol. J. Linn. Soc. 91 (4), 549–563. https://doi.org/10.1111/j.1095-8312.2007.00805.x.

Hundsdoerfer, A.K., Lee, K.M., Kitching, I.J., Mutanen, M., 2019. Genome-wide SNP data reveal an overestimation of species diversity in a group of hawkmoths. Genome biology and evolution 11 (8), 2136–2150. https://doi.org/10.1093/gbe/evz113.

Jackson, N.D., Carstens, B.C., Morales, A.E., O'Meara, B.C., 2017. Species delimitation with gene flow. Syst. Biol. 66 (5), 799–812. https://doi.org/10.1093/sysbio/syw117.

Jarvis, E.D., Mirarab, S., Aberer, A.J., Li, B., Houde, P., Li, C., Zhang, G., 2014. Whole-genome analyses resolve early branches in the tree of life of modern birds. Science 346 (6215), 1320–1331. https://doi.org/10.1126/science.1253451.

Jennings, W.B., Edwards, S.V., 2005. Speciational history of Australian grass finches (*Poephila*) inferred from thirty gene trees. Evolution 59 (9), 2033–2047. https://doi.org/10.1111/j.0014-3820.2005.tb01072.x.

Kalyaanamoorthy, S., Minh, B.Q., Wong, T.K.F., von Haeseler, A., Jermiin, L.S., 2017. ModelFinder: fast model selection for accurate phylogenetic estimates. Nat. Methods 14 (6), 587–589. https://doi.org/10.1038/nmeth.4285.

Kearns, A.M., Joseph, L., Omland, K.E., Cook, L.G., 2011. Testing the effect of transient Plio-Pleistocene barriers in monsoonal Australo-Papua: did mangrove habitats maintain genetic connectivity in the Black Butcherbird? Mol. Ecol. 20 (23), 5042–5059. https://doi.org/10.1111/j.1365-294X.2011.05330.x.

Keogh, J.S., Scott, I.A.W., Hayes, C., 2005. Rapid and repeated origin of insular gigantism and dwarfism in Australian tiger snakes. Evolution 59 (1), 226–233. https://doi.org/10.1554/04-310.

Kilian, A., Wenzl, P., Huttner, E., Carling, J., Xia, L., Blois, H., Caig, V., Heller-Uszynska, K., Jaccoud, D., Hopper, C., Aschenbrenner-Kilian, M., Evers, M., Peng, K., Cayla, C., Hok, P., Uszynski, G., 2012. Diversity arrays technology: a generic genome profiling technology on open platforms. Methods Mol. Biol. 888, 67–89. https://doi.org/10.1007/978-1-61779-870-2_5.

King, M., 2004. *Varanus baritji*. In: Pianka, E.R., King, D.R. (Eds.), Varanoid lizards of the world. Indiana University Press.

King, M., Horner, P., 1987. A new species of monitor (Platynota: Reptilia) from northern Australia and a note on the status of *Varanus acanthurus insulanicus* Mertens. The Beagle 4 (1), 73–79. https://doi.org/10.5962/p.260898.

Lanfear, R., Frandsen, P.B., Wright, A.M., Senfeld, T., Calcott, B., 2017. PartitionFinder 2: new methods for selecting partitioned models of evolution for molecular and morphological phylogenetic analyses. Mol. Biol. Evol. 34 (3), 772–773. https://doi.org/10.1093/molbev/msw260.

Laver, R.J., Doughty, P., Oliver, P.M., 2018. Origins and patterns of endemic diversity in two specialized lizard lineages from the Australian Monsoonal Tropics (*Oedura* spp.). J. Biogeogr. 45 (1), 142–153. https://doi.org/10.1111/jbi.13127.

Leaché, A.D., Banbury, B.L., Linkem, C.W., Nieto-Montes de Oca, A., 2016. Phylogenomics of a rapid radiation: is chromosomal evolution linked to increased diversification in north american spiny lizards (genus *Sceloporus*)? BMC Evol. Biol. 16 (1), 1–16. https://doi.org/10.1186/s12862-016-0628-x.

Leaché, A.D., Fujita, M.K., Minin, V.N., Bouckaert, R.R., 2014. Species delimitation using genome-wide SNP data. Syst. Biol. 63 (4), 534–542. https://doi.org/10.1093/sysbio/syu018.

Leaché, A.D., Zhu, T., Rannala, B., Yang, Z., 2019. The spectre of too many species. Syst. Biol. 68 (1), 168–181. https://doi.org/10.1093/sysbio/syy051.

Lewis, P.O., 2001. A likelihood approach to estimating phylogeny from discrete morphological character data. Syst. Biol. 50 (6), 913–925. https://doi.org/10.1080/106351501753462876.

Lind, A.L., Lai, Y.Y., Mostovoy, Y., Holloway, A.K., Iannucci, A., Mak, A.C., Bruneau, B. G., 2019. Genome of the Komodo dragon reveals adaptations in the cardiovascular and chemosensory systems of monitor lizards. Nat. Ecol. Evol. 3 (8), 1241–1252. https://doi.org/10.1038/s41559-019-0945-8.

Marshall, T.L., Chambers, E.A., Matz, M.V., Hillis, D.M., 2021. How mitonuclear discordance and geographic variation have confounded species boundaries in a widely studied snake. Mol. Phylogenet. Evol. 162, 107194 https://doi.org/10.1016/j.ympev.2021.107194.

Martin, H.A., 2006. Cenozoic climatic change and the development of the arid vegetation in Australia. J. Arid Environ. 66 (3), 533–563. https://doi.org/10.1016/j.jaridenv.2006.01.009.

McArthur River Mining. (2011). McArthur River Mine Phase 3 Development Project. Xstrata Zinc.

McLaren, S., Wallace, M.W., 2010. Plio-Pleistocene climate change and the onset of aridity in southeastern Australia. Global Planet. Change 71 (1–2), 55–72. https://doi.org/10.1016/J.GLOPLACHA.2009.12.007.

Melville, J., Haines, M.L., Boysen, K., Hodkinson, L., Kilian, A., Date, K.L.S., Potvin, D.A., Parris, K.M., 2017. Identifying hybridization and admixture using SNPs: application of the DArTseq platform in phylogeographic research on vertebrates. R. Soc. Open Sci. 4 (7) https://doi.org/10.1098/rsos.161061.

Mertens, R., 1958. Bemerkungen über die Warane Australiens. Senckenbergiana Biologica 39, 229–264.

Morales-Briones, D.F., Kadereit, G., Tefarikis, D.T., Moore, M.J., Smith, S.A., Brockington, S.F., Yang, Y., 2021. Disentangling sources of gene tree discordance in phylogenomic data sets: testing ancient hybridizations in Amaranthaceae sl. Syst. Biol. 70 (2), 219–235. https://doi.org/10.1093/sysbio/syaa066.

Moritz, C., Fujita, M.K., Rosauer, D., Agudo, R., Bourke, G., Doughty, P., Palmer, R., Pepper, M., Potter, S., Pratt, R., Scott, M., Tonione, M., Donnellan, S., 2016. Multilocus phylogeography reveals nested endemism in a gecko across the monsoonal tropics of Australia. Mol. Ecol. 25 (6), 1354–1366. https://doi.org/10.1111/mec.13511.

Mosimann, J.E., 1970. Size allometry: size and shape variables with characterizations of the lognormal and generalized gamma distributions. J. Am. Stat. Assoc. 65 (330), 930–945. https://doi.org/10.2307/2284599.

Moyle, R.G., Oliveros, C.H., Andersen, M.J., Hosner, P.A., Benz, B.W., Manthey, J.D., Faircloth, B.C., 2016. Tectonic collision and uplift of Wallacea triggered the global songbird radiation. Nat. Commun. 7 (1), 1–7. https://doi.org/10.1038/ncomms12709.

Nguyen, L.-T., Schmidt, H.A., von Haeseler, A., Minh, B.Q., 2015. IQ-TREE: a fast and effective stochastic algorithm for estimating maximum-likelihood phylogenies. Mol. Biol. Evol. 32 (1), 268–274. https://doi.org/10.1093/molbev/msu300.

Noble, C., Laver, R.J., Rosauer, D.F., Ferrier, S., Moritz, C., 2018. Phylogeographic evidence for evolutionary refugia in the Gulf sandstone ranges of northern Australia. Aust. J. Zool. 65 (6), 408–416. https://doi.org/10.1071/ZO17079.

Noguerales, V., Cordero, P.J., Ortego, J., 2018. Integrating genomic and phenotypic data to evaluate alternative phylogenetic and species delimitation hypotheses in a recent evolutionary radiation of grasshoppers. Mol. Ecol. 27 (5), 1229–1244. https://doi.org/10.1111/mec.14504.

Oliver, P.M., Ashman, L.G., Bank, S., Laver, R.J., Pratt, R.C., Tedeschi, L.G., Moritz, C.C., 2019. On and off the rocks: persistence and ecological diversification in a tropical Australian lizard radiation. BMC Evol. Biol. 19 (1), 1–15. https://doi.org/10.1186/s12862-019-1408-1.

Oliver, P.M., Couper, P.J., Pepper, M., 2014. Independent transitions between monsoonal and arid biomes revealed by systematic revison of a complex of Australian geckos (*Diplodactylus*; Diplodactylidae). PLoS ONE 9 (12), e111895. https://doi.org/10.1371/journal.pone.0111895.

Oliver, P.M., Laver, R.J., De Mello Martins, F., Pratt, R.C., Hunjan, S., Moritz, C.C., 2017. A novel hotspot of vertebrate endemism and an evolutionary refugium in tropical Australia. Divers. Distrib. 23 (1), 53–66. https://doi.org/10.1111/ddi.12506.

One Thousand Plant Transcriptomes Initiative, 2019. One thousand plant transcriptomes and the phylogenomics of green plants. Nature 574, 679–685. https://doi.org/10.1038/s41586-019-1693-2.

Pante, E., Puillandre, N., Viricel, A., Arnaud-Haond, S., Aurelle, D., Castelin, M., Samadi, S., 2015. Species are hypotheses: avoid connectivity assessments based on pillars of sand. Mol. Ecol. 24 (3), 525–544. https://doi.org/10.1111/mec.13048.

Pavón-Vázquez, C.J., Brennan, I.G., Skeels, A., Keogh, J.S., 2022. Competition and geography underlie speciation and morphological evolution in Indo-Australasian monitor lizards. Evolution 76 (3), 476–495. https://doi.org/10.1111/evo.14403.

Pepper, M., Keogh, J.S., 2021. Life in the "dead heart" of Australia: The geohistory of the Australian deserts and its impact on genetic diversity of arid zone lizards. J. Biogeogr. 48 (4), 716–746. https://doi.org/10.1111/jbi.14063.

Pepper, M., Doughty, P., Keogh, J.S., 2013. Geodiversity and endemism in the iconic Australian Pilbara region: a review of landscape evolution and biotic response in an ancient refugium. J. Biogeogr. 40 (7), 1225–1239. https://doi.org/10.1111/jbi.12080.

Pepper, M., Fujita, M.K., Moritz, C., Keogh, J.S., 2011a. Palaeoclimate change drove diversification among isolated mountain refugia in the Australian arid zone. Mol. Ecol. 20 (7), 1529–1545. https://doi.org/10.1111/j.1365-294x.2011.05036.x.

Pepper, M., Ho, S.Y., Fujita, M.K., Keogh, J.S., 2011b. The genetic legacy of aridification: climate cycling fostered lizard diversification in Australian montane refugia and left low-lying deserts genetically depauperate. Mol. Phylogenet. Evol. 61 (3), 750–759. https://doi.org/10.1016/j.ympev.2011.08.009.

Petroli, C. D., Sansaloni, C. P., Carling, J., Steane, D. A., Vaillancourt, R. E., Myburg, A. A., Bonfim da Silva Jr., O., Pappas Jr., G. J., Kilian, A., & Grattapaglia, D. (2012). Genomic characterization of DArT markers based on high-density linkage analysis and physical mapping to the *Eucalyptus* genome. PLoS One, 7(9), e44684. https://doi.org/10.1371/journal.pone.0044684.

Pianka, E., King, D. (Eds.), 2004. Varanoid lizards of the world. Indiana University Press. https://doi.org/10.2307/j.ctt2005wjp.

Potter, S., Bragg, J.G., Peter, B.M., Bi, K., Moritz, C., 2016. Phylogenomics at the tips: inferring lineages and their demographic history in a tropical lizard. *Carlia amax*. Mol. Ecol. 25 (6), 1367–1380. https://doi.org/10.1111/mec.13546.

Potter, S., Cooper, S.J.B., Metcalfe, C.J., Taggart, D.A., Eldridge, M.D.B., 2012. Phylogenetic relationships of rock-wallabies, *Petrogale* (Marsupialia: Macropodidae) and their biogeographic history within Australia. Mol. Phylogenet. Evol. 62 (2), 640–652. https://doi.org/10.1016/j.ympev.2011.11.005.

Powney, G.D., Grenyer, R., Orme, C.D.L., Owens, I.P.F., Meiri, S., 2010. Hot, dry and different: Australian lizard richness is unlike that of mammals, amphibians and birds. Global Ecol. Biogeogr. 19 (3), 386–396. https://doi.org/10.1111/j.1466-8238.2009.00521.x.

R Core Team, 2019. R: A language and environment for statistical computing. R Foundation for Statistical Computing, Vienna, Austria. Available at: https://www.R-project.org/.

Rambaut, A., Suchard, M. A., Xie, D., & Drummond, A. J. (2014). Tracer v1.6. Available at: http://beast.bio.ed.ac.uk/Tracer.

Ritchie, M.G., Hamill, R.M., Graves, J.A., Magurran, A.E., Webb, S.A., Garcia, C.M., 2007. Sex and differentiation: population genetic divergence and sexual dimorphism in Mexican goodeid fish. J. Evol. Biol. 20 (5), 2048–2055. https://doi.org/10.1111/j.1420-9101.2007.01357.x.

Roulin, A., & Salamin, N. (2010). Insularity and the evolution of melanism, sexual dichromatism and body size in the worldwide-distributed barn owl. J. Evol. Biol., 23 (5), 925–934. https://doi.org/10.1111/j.1420-9101.2010.01961.x.

Rousset. (2000). Genetic differentiation between individuals. J. Evol. Biol., 13(1), 58–62. https://doi.org/10.1046/j.1420-9101.2000.00137.x.

Rutherford, S., Rossetto, M., Bragg, J.G., McPherson, H., Benson, D., Bonser, S.P., Wilson, P.G., 2018. Speciation in the presence of gene flow: population genomics of closely related and diverging *Eucalyptus* species. Heredity 121 (2), 126–141. https://doi.org/10.1038/s41437-018-0073-2.

Schmida, G., 2020. A photographic guide to Australian monitors. Blurb.

Sexton, J.P., Hangartner, S.B., Hoffmann, A.A., 2014. Genetic isolation by environment or distance: which pattern of gene flow is most common? Evolution 68 (1), 1–15. https://doi.org/10.1111/evo.12258.

Slatyer, C., Rosauer, D., Lemckert, F., 2007. An assessment of endemism and species richness patterns in the Australian Anura. J. Biogeogr. 34 (4), 583–596. https://doi.org/10.1111/j.1365-2699.2006.01647.x.

Smith, K.L., Harmon, L.J., Shoo, L.P., Melville, J., 2011. Evidence of constrained phenotypic evolution in a cryptic species complex of agamid lizards. Evolution 65 (4), 976–992. https://doi.org/10.1111/j.1558-5646.2010.01211.x.

Stammer, D., 1970. Goannas. Wildl. Austr. 7, 118–120.

Stange, M., Sánchez-Villagra, M.R., Salzburger, W., Matschiner, M., 2018. Bayesian divergence-time estimation with genome-wide single-nucleotide polymorphism data of sea catfishes (Ariidae) supports Miocene closure of the Panamanian Isthmus. Syst. Biol. 67 (4), 681–699. https://doi.org/10.1093/sysbio/syy006.

Stanton, D.W., Frandsen, P., Waples, R.K., Heller, R., Russo, I.R.M., Orozco-terWengel, P. A., Bruford, M.W., 2019. More grist for the mill? Species delimitation in the genomic era and its implications for conservation. Conserv. Genet. 20 (1), 101–113. https://doi.org/10.1007/s10592-019-01149-5.

Stekhoven, D.J., Bühlmann, P., 2012. MissForest—non-parametric missing value imputation for mixed-type data. Bioinformatics 28 (1), 112–118. https://doi.org/10.1093/bioinformatics/btr597.

Storr, G.M., 1966. Rediscovery and taxonomic status of the Australian lizard *Varanus primordius*. Copeia 1966 (3), 583–584. https://doi.org/10.2307/1441088.

Storr, G.M., 1980. The monitor lizards (genus *Varanus* Merrem, 1820) of Western Australia. Rec. West. Aust. Mus. 8 (2), 237–293.

Streicher, J.W., Wiens, J.J., 2017. Phylogenomic analyses of more than 4000 nuclear loci resolve the origin of snakes among lizard families. Biol. Lett. 13 (9), 20170393. https://doi.org/10.1098/rsbl.2017.0393.

Suh, A., 2016. The phylogenomic forest of bird trees contains a hard polytomy at the root of Neoaves. Zoolog. Scr. 45, 50–62. https://doi.org/10.1111/zsc.12213.

Swanson, S., 1979. Some rock-dwelling reptiles of the Arnhem Land escarpment. Northern Territory Naturalist 1979, 14–18.

Swofford, D. L. (2003) PAUP*. Phylogenetic analysis using parsimony and other methods. Version 4. Sinauer Associates.

Tarver, J.E., Dos Reis, M., Mirarab, S., Moran, R.J., Parker, S., O'Reilly, J.E., Pisani, D., 2016. The interrelationships of placental mammals and the limits of phylogenetic inference. Genome biology and evolution 8 (2), 330–344. https://doi.org/10.1093/gbe/evv261.

Thompson, G.G., Clemente, C.J., Withers, P.C., Fry, B.G., Norman, J.A., 2009. Is body shape of varanid lizards linked with retreat choice? Aust. J. Zool. 56 (5), 351–362. https://doi.org/10.1071/ZO08030.

Tsagkogeorga, G., Parker, J., Stupka, E., Cotton, J.A., Rossiter, S.J., 2013. Phylogenomic analyses elucidate the evolutionary relationships of bats. Curr. Biol. 23 (22), 2262–2267. https://doi.org/10.1016/j.cub.2013.09.014.

Vidal, N., Marin, J., Sassi, J., Battistuzzi, F.U., Donnellan, S., Fitch, A.J., Fry, B.G., Vonk, F.J., Rodriguez de la Vega, R.C., Couloux, A., Hedges, S.B., 2012. Molecular evidence for an Asian origin of monitor lizards followed by Tertiary dispersals to Africa and Australasia. Biol. Lett. 8 (5), 853–855. https://doi.org/10.1098/rsbl.2012.0460/.

Wilson, S.K., Swan, G., 2021. A complete guide to reptiles of Australia, sixth ed. Reed New Holland.

Zhu, X.-M., Du, Y., Qu, Y.-F., Li, H., Gao, J.-F., Lin, C.-X., Lin, L.-H., 2020. The geographical diversification in varanid lizards: the role of mainland versus island in driving species evolution. Curr. Zool. 66 (2), 165–171. https://doi.org/10.1093/cz/zoaa002.